



HAL
open science

Digital Planarity - A Review

Valentin Brimkov, David Coeurjolly, Reihnard Klette

► **To cite this version:**

Valentin Brimkov, David Coeurjolly, Reihnard Klette. Digital Planarity - A Review. *Discrete Applied Mathematics*, 2007, 155 (4), pp.468-495. 10.1016/j.dam.2006.08.004 . hal-00185059

HAL Id: hal-00185059

<https://hal.science/hal-00185059>

Submitted on 6 Nov 2007

HAL is a multi-disciplinary open access archive for the deposit and dissemination of scientific research documents, whether they are published or not. The documents may come from teaching and research institutions in France or abroad, or from public or private research centers.

L'archive ouverte pluridisciplinaire **HAL**, est destinée au dépôt et à la diffusion de documents scientifiques de niveau recherche, publiés ou non, émanant des établissements d'enseignement et de recherche français ou étrangers, des laboratoires publics ou privés.

Digital Planarity - A Review

Valentin Brimkov,^{a,1} David Coeurjolly,^b and Reinhard Klette^c

^a*Mathematics Department, SUNY Buffalo State College, Buffalo, NY 14222, USA*

^b*LIRIS, CNRS UMR 5205, Université Claude Bernard Lyon 1, F-69622
Villeurbanne, France*

^c*Computer Science Department, The University of Auckland, New Zealand*

Abstract

Digital planarity is defined by digitizing Euclidean planes in the three-dimensional digital space of voxels; voxels are given either in the grid-point or the grid-cube model. The paper summarizes results (also including most of the proofs) about different aspects of digital planarity, such as supporting or separating Euclidean planes, characterizations in arithmetic geometry, periodicity, connectivity, and algorithmic solutions. The paper provides a uniform presentation, which further extends and details a recent book chapter in (Klette and Rosenfeld 2004).

Key words: digital planes, digital geometry, arithmetic geometry, 2D array
periodicity, Sturmian words, geometric algorithms
1991 MSC: 52C99, 62H35, 65D18, 68U05

1 Introduction

In this paper we review various concepts and results of digital planarity and exhibit relations of the subject to other disciplines. Some of the considered subjects are partially familiar from studies on digital straightness. However, digital planarity issues appear to be more challenging, due to interesting applications in three-dimensional (3D) pattern recognition or volume modeling, and to theoretical difficulties caused by dealing with a discrete two-dimensional (2D) manifold in a discrete 3D space.

¹ On leave from the Institute of Mathematics and Computer Science, Bulgarian Academy of Sciences, 1113 Sofia, Bulgaria.

We conform to traditional terminology adopted in digital geometry, following (Klette and Rosenfeld 2004). Various basic notions (such as digital connectivity, gap or gap-freeness, and so forth) will be introduced along with the digital planarity aspects to be considered. 2D digital geometry deals with sets of *pixels*, represented either by grid points (defined by integer coordinates) or unit grid cells in the plane, also called *2-cells*. 3D digital geometry deals with sets of *voxels*, represented either in a 3D *grid-point* or *grid-cube* model. Although both models are basically equivalent, they provide frameworks for elucidating specific aspects of digital planarity. In the grid-point model, a digital 3D object (i.e., a finite or infinite set of voxels) is a set of grid points (x, y, z) in the uniform orthogonal grid (i.e., x, y , and z are integers); in the grid-cube model it is a set of unit grid cubes, also called *3-cells*, where each grid cube has a grid point as its center point. Note that in both models a voxel is uniquely identified by one grid point. We also use m -cells, with $0 \leq m < 3$; the frontier of a 3-cell contains six *2-cells*, twelve *1-cells*, and eight *0-cells*. (Generalizations of these notions to arbitrary $n > 0$ dimensions are straightforward.)

A grid-point or grid-cube space is equipped with a symmetric and irreflexive adjacency relation. Let $n = 2$ or $n = 3$. Two n -cells are called *m-adjacent* iff their intersection contains an m -cell, for $0 \leq m < n$. Two n -cells c_1 and c_2 are *m-neighbors* iff $c_1 = c_2$, or they are *m-adjacent*. The grid-point model prefers terminology based on cardinalities: two 2D grid points are 4-adjacent (8-adjacent) iff they are centers of two 2-cells which are 1-adjacent (0-adjacent); two 3D grid points are 6-adjacent (18- or 26-adjacent) iff they are centers of two 3-cells which are 2-adjacent (1- or 0-adjacent). In this paper we prefer to use the grid-cube model rather than the grid-point model.

A set S of pixels or voxels is *α -connected* iff for any pair $c_1, c_2 \in S$ there is an α -path $p_1 = c_1, p_2, \dots, p_n = c_2$, with $p_i \in S$ for $i = 1, \dots, n$, and p_{i+1} is α -adjacent to p_i for $i = 1, \dots, n - 1$. An *α -component* of a set M of pixels or voxels is a maximal (by inclusion) α -connected subset of M ; it is an *α -region* if it is also finite.

Two cells c_1 and c_2 are *incident* iff c_1 is a subset of c_2 , or vice versa. Let $\mathbb{C}_3^{(m)}$

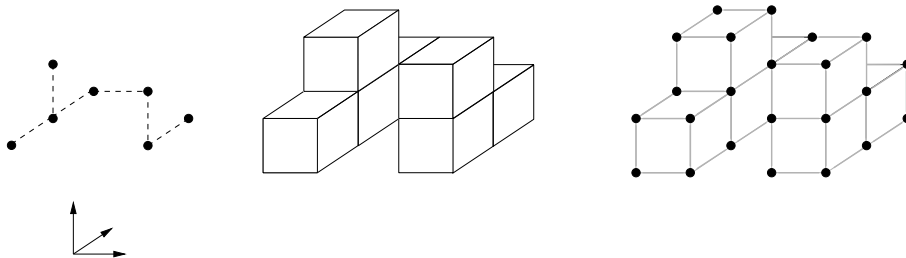


Fig. 1. Example of a set of voxels represented in the grid-point model (*left*), the grid-cube model (*middle*), and the incidence grid (*right*).

be the class of all m -cells in \mathbb{R}^3 , for $m = 0, 1, 2, 3$. The *incidence grid* \mathbb{C}_3 is defined by these classes and the incidence relation. For example, a single 1-cell c (i.e., a grid edge in $\mathbb{C}_3^{(1)}$) is incident with exactly two 0-cells (i.e., grid vertices), one 1-cell (the grid edge c itself), four 2-cells (i.e., grid squares), and four 3-cells (i.e., grid cubes). Using these notations, the grid-cube model (as defined above) is $\mathbb{C}_3^{(3)}$ combined with an adjacency relation. Figure 1 illustrates the different models.

1.2 Digital planes

We consider a Euclidean plane Γ in \mathbb{R}^3 defined by an equation

$$a_1x + a_2y + a_3z = b \tag{1}$$

where $a_1, a_2, a_3, b \in \mathbb{R}$. The symmetry of the space \mathbb{R}^3 and of the integer grid allows us to assume without loss of generality (for discussions on theoretical properties of digital planes) that $0 \leq a_1 \leq a_2 \leq a_3 \neq 0$. Dividing both sides of (1) by a_3 , we obtain that

$$\Gamma(\alpha_1, \alpha_2, \beta) = \{(x, y, z) \in \mathbb{R}^3 : z = \alpha_1x + \alpha_2y + \beta\} \tag{2}$$

where $\alpha_1, \alpha_2, \beta \in \mathbb{R}$, $\alpha_1 = -a_1/a_3$, $\alpha_2 = -a_2/a_3$, and $\beta = b/a_3$, with

$$0 \leq \alpha_1 \leq 1 \quad \text{and} \quad 0 \leq \alpha_2 \leq 1 \tag{3}$$

Throughout this paper we can also assume that

$$0 \leq \beta < 1 \tag{4}$$

because planes, whose intercepts β differ by an integer, possess digitizations with equivalent properties in all categories reviewed in this paper.

We define a digital plane with respect to a model of digitization. Simplifying but popular models are: **(i)** *3D grid-line intersection digitization* which assigns all those 3D grid points which are nearest (if two at equal distance, then the one further away from the origin) to an intersection of the plane to be digitized with any of the grid lines, **(ii)** *outer 3D Jordan digitization* (also known as *supercover digitization*) which assigns all those grid cubes having a non-empty intersection with the given plane, or **(iii)** digitizations which simply apply the floor, closest-integer, or ceiling function to the coordinates of the points in $\Gamma(\alpha_1, \alpha_2, \beta)$. For a detailed description of digitization models the reader is referred to (Klette and Rosenfeld 2004).

Assume grid-line intersection digitization and the 3D grid-point model. Under assumptions (3) and (4) for $\alpha_1, \alpha_2, \beta$, it is sufficient to consider only intersections with grid lines parallel to the z -axis.

Definition 1 Let $\Gamma(\alpha_1, \alpha_2, \beta)$ intersect the vertical grid line, defined by $x = m$ and $y = n$, at $p_{m,n}$, where $m, n \geq 0$. Let $(m, n, I_{m,n})$ be the grid point closest to $p_{m,n}$. Then a *digital plane quadrant* is a set of grid points which is defined as follows:

$$I_{\alpha_1, \alpha_2, \beta} = \{(m, n, I_{m,n}) : m, n \geq 0 \wedge I_{m,n} = \lfloor \alpha_1 m + \alpha_2 n + \beta + 0.5 \rfloor\}$$

If m, n are not required to be nonnegative, we have a *digital plane*. If α_1 or α_2 is irrational, then we speak about an *irrational digital plane quadrant* (*irrational digital plane*); otherwise it is a *rational digital plane quadrant* (*rational digital plane*).

Note that in the above formula adding 0.5 to $\alpha_1 m + \alpha_2 n + \beta$ assures that if there are two closest grid points, then always the upper one is chosen.

The set $I_{\alpha_1, \alpha_2, \beta}$ uniquely determines both the slopes α_1 and α_2 and the intercept β if α_1 or α_2 is irrational. If both α_1 and α_2 are rational, $I_{\alpha_1, \alpha_2, \beta}$ uniquely determines α_1 and α_2 , but determines β only up to an interval. This can be proved by a 3D generalization of the proof of Bruckstein's theorem (Bruckstein 1991) as stated in (Rosenfeld and Klette 2001).

For discussing digital planarity exclusively within the grid-cube model, we can uniquely identify each grid point (in a digital plane as defined above) as being the centroid of a grid cube. This way, a *cellular digital plane* is defined by a digital plane in the grid-point model. (Alternatively, a cellular digital plane could also be defined by outer Jordan digitization of a plane Γ . However, if Γ passes through a grid vertex or contains a grid edge, then outer Jordan digitization would produce “locally thicker” cellular planes).

The grid-cube model also allows to introduce further notions in the context of digital planarity. Consider the union of all grid cubes contained in a set of voxels. Its topological frontier (within the Euclidean topology of \mathbb{R}^3) consists of 2-cells called *frontier faces*. The frontier faces of a cellular digital plane define an *upper* and a *lower digital frontier plane* in the incidence grid \mathbb{C}_3 . (Note that these are analogous to lower and upper digital lines defined in (Rosenfeld and Klette 2001) for the study of digital straightness.). Upper and lower digital frontier planes share in general 0- and 1-cells, but not 2-cells.

Definition 2 A set $S \subset \mathbb{C}_3^{(2)}$ of 2-cells in the incidence grid is called a *digital plane of 2-cells* iff it is either an upper or a lower digital frontier plane defined by a cellular digital plane.

1.3 Digital surface and surface patch

A digital plane is a special case of a digital surface. For a brief survey on digital surfaces, see (Brimkov and Klette 2004). Below we present an early definition of a digital surface, and a (historically early) theorem characterizing any digital plane as a digital surface.

Let S be a set of voxels. We define *slices* $S_{x=i} = \{(i, y, z) \in S : y, z \in \mathbb{Z}\}$, $S_{y=j} = \{(x, j, z) \in S : x, z \in \mathbb{Z}\}$, and $S_{z=k} = \{(x, y, k) \in S : x, y \in \mathbb{Z}\}$.

Definition 3 (Kim 1984) A 0-connected set $S \subseteq \mathbb{C}_3^{(3)}$ is called a *digital surface* iff each 3-cell $p = (i, j, k) \in S$ has at most two 0-adjacent 3-cells in at least two of the slices $S_{x=i}$, $S_{y=j}$, or $S_{z=k}$; if it has two, then they are not mutually 0-adjacent; and if p has in one of these sets, say, in $S_{z=k}$, more than two 0-adjacent 3-cells, or two 0-adjacent 3-cells that are mutually 0-adjacent, then there is no $(i, j, k - 1)$ or $(i, j, k + 1)$ in S .

Theorem 4 (Kim 1984) A (cellular) digital plane is an unbounded digital surface.

PROOF. Let $p = (i, j, k)$ be a voxel of a digital plane $I_{\alpha_1, \alpha_2, \beta}$, and consider $I_{\alpha_1, \alpha_2, \beta} \cap S_{x=i}$. Let $p' = (i, j - 1, k')$ and $p'' = (i, j + 1, k'')$ be the only two voxels of $I_{\alpha_1, \alpha_2, \beta}$ with centers on the vertical lines $x = i$ and $y = j - 1$ and $x = i$ and $y = j + 1$, respectively. Since $\alpha_1 \leq \alpha_2$, we have $0 \leq |k - k'|, |k - k''| \leq 1$. Thus $(i, j - 1, k')$ and $(i, j + 1, k'')$ are the only two voxels defined by p and $x = i$, which are 0-adjacent to (i, j, k) , but not mutually 0-adjacent. Similarly, p and $y = j$ define only two 0-adjacent voxels in $I_{\alpha_1, \alpha_2, \beta} \cap S_{y=j}$, which are not mutually 0-adjacent. In $I_{\alpha_1, \alpha_2, \beta} \cap S_{z=k}$, p and $z = k$ may define more than two 0-adjacent voxels. However, $(i, j, k - 1)$ and $(i, j, k + 1)$ are not both in $I_{\alpha_1, \alpha_2, \beta}$ since $p = (i, j, k)$ is the only voxel of $I_{\alpha_1, \alpha_2, \beta}$ with a center on the vertical grid line $x = i$ and $y = j$. Thus it follows that $I_{\alpha_1, \alpha_2, \beta}$ is a digital surface. \square

A voxel $p = (i, j, k)$ of a digital surface S is called a *border voxel* of S iff it has only one 0-neighbor in at least one of the slices $S_{x=i}$, $S_{y=j}$, or $S_{z=k}$. p is called an *inner voxel* of S iff it is not a border voxel. A *simple digital surface* is a digital surface that has no border voxels; it can be either unbounded or bounded. A *digital surface patch* (Kim 1984) is a finite digital surface whose border voxels are all (at least) 0-connected (see Figure 2).

Definition 5 Let $D \subset \mathbb{Z}^2$ be a 1-region. Then $I_{\alpha_1, \alpha_2, \beta}^D$ is called a *digital plane segment (DPS)*. In the 3D incidence grid model, a DPS of 2-cells is given by a finite 1-connected subset of a digital plane of 2-cells.

Corollary 6 A digital plane segment $I_{\alpha_1, \alpha_2, \beta}^D$ is a digital surface patch.

In the following sections we review concepts and results related to digital planarity. The paper is structured as follows. In Section 2, we give some alternative definitions in terms of the chordal triangle property and evenness of surfaces. In Section 3, we characterize digital planes through supporting and separating planes, as well as in the framework of arithmetic geometry. In Section 4, we introduce height and remainder maps that are instrumental in studying periodicity and connectivity properties of digital planes. In Section 5, we review results on digital plane periodicity, while in Section 6 we address connectivity issues. In Section 7, we summarize a few algorithms for digital plane recognition, digital surface segmentation, and polyhedral surface generation. We conclude with some final remarks in Section 8.

2 Alternative Definitions

We use the Minkowski metric L_∞ . If applied to \mathbb{Z}^3 , it is identical to the grid point metric d_{26} , i.e., we have $d_{26}(p, q) = L_\infty(p, q) = \max\{|x_1 - x_2|, |y_1 - y_2|, |z_1 - z_2|\}$ for any $p, q \in \mathbb{R}^3$, with $p = (x_1, y_1, z_1)$, and $q = (x_2, y_2, z_2)$.

Definition 7 (Kim and Rosenfeld 1982) $S \subseteq \mathbb{Z}^3$ is said to have the *chordal triangle property* iff for any $p_1, p_2, p_3 \in S$, every point of the triangle $p_1p_2p_3 \subset \mathbb{R}^3$ is at L_∞ -distance < 1 from some point of S .

Obviously, a simple digital surface which satisfies the chordal property cannot be bounded.

Theorem 8 (Kim 1984) *A simple digital surface is a digital plane iff it has the chordal triangle property.*

The original proof is too long to be part of this review, therefore we only sketch it. First, Kim shows that, given a digital plane, there is a coordinate plane (the plane $z = 0$ according to our assumptions (3), (4)) such that the projection of the digital plane onto its grid points is a one-to-one and onto mapping (Kim 1984, Lemma 9). This lemma allows to reduce the dimension of

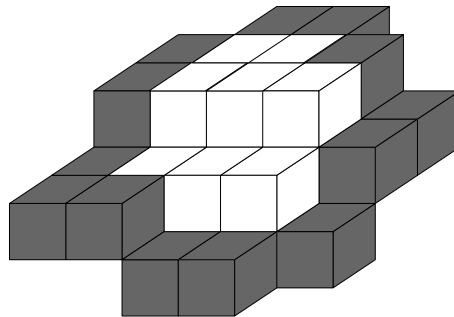


Fig. 2. Example of a digital surface patch; border voxels are shown in gray, and inner voxels in white.

the considered problem and to perform all considerations in such a coordinate plane rather than in 3D. Then the first implication (a digital plane has the chordal triangle property) can be easily derived (Kim 1984, Lemma 10). A key point is the existence of a Euclidean plane $\Gamma_{\alpha_1, \alpha_2, \beta}$ defining the given digital plane.

The proof of the converse proposition (a simple digital surface with the chordal triangle property is a digital plane) is more complicated. As a first step, it is shown that if a simple digital surface has the chordal triangle property, then there is a one-to-one and onto coordinate projection plane (Kim 1984, Lemma 11). Then the proof is completed by exhaustive analysis of different cases, conditioned by the distance between the supporting plane of a triangle and the points of the simple digital surface (Kim 1984, Lemma 12).

For any $p = (p_x, p_y, p_z) \in \mathbb{Z}^3$, let $p_{z=0} = (p_x, p_y, 0)$ be the projection of p onto the xy -plane.

Definition 9 $S \subseteq \mathbb{Z}^3$ is called *even* iff its projection onto the xy -plane $\mathbb{Z}_{z=0}^3$ is one-to-one, and for every quadruple (p, q, r, s) of points in S such that $p_{z=0} - q_{z=0} = r_{z=0} - s_{z=0}$, we have $|(p_z - q_z) - (r_z - s_z)| \leq 1$.

Defining evenness with respect to the xy -plane is consistent with our assumptions (3), (4). By requiring a one-to-one mapping onto the xy -plane, we consider only unbounded sets $S \subseteq \mathbb{Z}^3$ as being even. The following theorem does not make use of our general assumption that $\alpha_1 \leq \alpha_2$.

Theorem 10 (Veelaert 1993) *A simple digital surface is a digital plane iff it has the evenness property.*

Again we only sketch the original proof. As a first step, digital planarity is characterized in terms of linear programming: a set S of voxels is a subset of a digital plane if there exist $(\alpha_1, \alpha_2, \beta) \in [0, 1] \times [0, 1]^2$, such that

$$0 \leq \alpha_1 m + \alpha_2 n + \beta - I_{m,n} < 1$$

for all $(m, n, I_{m,n}) \in S$. Hence, to decide whether S is a subset of a digital plane, we have to solve a system of linear inequalities with unknowns α_1, α_2 , and β . Given a voxel $(m, n, I_{m,n})$, an elementary convex open set associated with it is defined by two linear inequalities in three unknowns. S is a subset of a digital plane if the intersection of these elementary convex open sets is non-empty.

Next, one takes advantage of the following fundamental theorem of Helly: Let \mathcal{F} be a finite family of $n + 1$ or more convex subsets of \mathbb{R}^n . If every

² Throughout by $]p, q[$, $[p, q]$, and $[p, q[$ we denote an open, a closed, and a semi-open interval, respectively.

subfamily, consisting of $n + 1$ sets of \mathcal{F} , has a non-empty intersection, then \mathcal{F} has a non-empty intersection. Thus, in dimension 3, the system induced by the elementary convex sets has a solution if and only if each subsystem with four inequalities has a solution.

Finally, Veelaert proves that the evenness criterion can be used as a ‘‘Helly subsystem criterion.’’ Note that the original result is valid for arbitrary dimensions. Moreover, it is shown that Kim’s chordal triangle property is actually another Helly criterion.

(Veelaert 1994) also shows that for some special types of finite sets S of voxels (e.g., such that the projection onto the xy -plane is a rectangle), S is a subset of a digital plane iff S is even.

3 Supporting and Separating Planes

A *supporting plane* of a set $S \subseteq \mathbb{Z}^3$ is a Euclidean plane that divides \mathbb{R}^3 into two (open) half-spaces such that S is completely contained in the closure of one of them. For the next theorem note that any metric in \mathbb{R}^3 induces a Hausdorff distance between subsets of \mathbb{R}^3 . We use the Minkowski metric L_∞ .

Theorem 11 (Kim 1984) *$S \subseteq \mathbb{Z}^3$ is a digital plane iff it has a supporting plane Γ such that the L_∞ -Hausdorff distance between S and Γ is less than 1.*

PROOF. Let $\Gamma(\alpha_1, \alpha_2, \beta)$ be a supporting plane for $S \subseteq \mathbb{Z}^3$ satisfying the hypothesis of the theorem to be proved. We assume without loss of generality that Γ is above S with respect to the z -axis. Let the L_∞ -Hausdorff distance between S and Γ be < 1 . Then the vertical distance from any point of S to Γ is < 1 , as well. Denote by Γ' the plane obtained by translating Γ by a vector $(0, 0, -\frac{1}{2})^T$. Then Γ' is such that $S \subset I_{\alpha_1, \alpha_2, \beta - \frac{1}{2}}$ and so, S is a digital plane. Conversely, suppose that S is a digital plane. Then there exists a plane $\Gamma(\alpha_1, \alpha_2, \beta)$ such that $S \subset I_{\alpha_1, \alpha_2, \beta}$. By definition of a digital plane, the vertical distance from any point of S to Γ is less than $\frac{1}{2}$. Let Γ' be the plane obtained by translation of Γ by a vector $(0, 0, \frac{1}{2})^T$. Then any point of S is below Γ' and the L_∞ -Hausdorff distance between S and Γ' is < 1 . Hence, Γ' is a supporting plane of S . \square

In (Kim 1984) it was claimed that if $S \subseteq \mathbb{Z}^3$ is a (finite) DPS, then the points of S are at L_∞ -Hausdorff distance < 1 from at least one Euclidean plane incident with one of the faces of the convex hull of S . Then one of these planes is a supporting plane in the sense of Theorem 11. However, (Debled-Rennesson 1995) gave a counter-example: for $D = [0, 6] \times [0, 7]$, the L_∞ -Hausdorff distance be-

tween $I_{5/29,9/29,1/2}^D$ and any plane incident with one of the faces of the convex hull of $I_{5/29,9/29,1/2}^D$ is greater than 1.

Let $S \subset \mathbb{Z}^3$ and $S_{z+1} = \{(i, j, k + 1) : (i, j, k) \in S\}$. A plane $\Gamma \subset \mathbb{R}^3$ *separates* the sets $S_1, S_2 \subset \mathbb{Z}^3$ iff S_1 and S_2 are in opposite open half-spaces defined by Γ .

Theorem 12 (Stojmenović and Tosić 1991) *A set $S \subset \mathbb{Z}^3$ is a subset of a digital plane iff there exists a plane that separates S from S_{z+1} .*

PROOF. We first suppose that S is a subset of a digital plane. Let $\Gamma(\alpha_1, \alpha_2, \beta)$ be the plane such that $S \subset I_{\alpha_1, \alpha_2, \beta}$ and Γ' the plane with parameters $(\alpha_1, \alpha_2, \beta + \frac{1}{2})$. We consider the points $r = (r_x, r_y, r_z) \in S$, $p = (r_x, r_y, p_z) \in \Gamma$, $p' = (r_x, r_y, p'_z) \in \Gamma'$, and $r_{z+1} = (r_x, r_y, r_z + 1) \in S_{z+1}$. From the definition of 3D grid-line intersection digitization and the definition of Γ' , it follows that $p'_z - 1 < r_z \leq p'_z < r_z + 1$. Hence, the number p'_z “separates” the numbers r and r_{z+1} . Since this property is valid for every point of S , it follows that Γ' separates S from S_{z+1} , even if S is not finite. Conversely, let $\Gamma(\alpha_1, \alpha_2, \beta)$ be a separating plane for S and S_{z+1} . We consider $r \in S$, $r_{z+1} = (r_x, r_y, r_z + 1) \in S_{z+1}$ and $p = (r_x, r_y, p_z) \in \Gamma$. We have $r_z \leq p_z < r_z + 1$, i.e., $r_z - \frac{1}{2} \leq p_z - \frac{1}{2} < r_z + \frac{1}{2}$. Thus we obtain that the digital image of Γ' with parameters $(\alpha_1, \alpha_2, \beta - \frac{1}{2})$ is such that $S \subset I_{\alpha_1, \alpha_2, \beta - \frac{1}{2}}$. This means that S is a subset of a digital plane. \square

Arithmetic geometry, as briefly indicated in (Forchhammer 1989) and developed in (Reveillès 1991), provides a uniform approach to the study of digitized hyperplanes in n dimensions. Basic definitions follow the general idea of specifying lower and upper supporting planes. We discuss here the three-dimensional case. Let a, b, c, μ , and $\omega \geq 0$ be integers.

Definition 13 $D_{a,b,c,\mu,\omega} = \{(i, j, k) \in \mathbb{Z}^3 : \mu \leq ai + bj + ck < \mu + \omega\}$ is called an *arithmetic plane* with *normal* $\mathbf{n} = (a, b, c)^T$, *intercept* μ , and *arithmetic thickness* ω .

An arithmetic plane is a generalization of an arithmetic line $D_{a,b,\mu,\omega} = \{(i, j) \in \mathbb{Z}^2 : \mu \leq ai + bj < \mu + \omega\}$. From Reveillès’ theorem on arithmetic lines (Reveillès 1991) we know that *naive lines* (with $\omega = \max\{|a|, |b|\}$) are the same as digital lines (which are 0-paths), and *standard lines* (with $\omega = |a| + |b|$) are the same as upper or lower digital lines (which are 1-paths, see (Rosenfeld and Klette 2001)). If $\omega = \max\{|a|, |b|, |c|\}$, then the arithmetic plane $D_{a,b,c,\mu,\omega}$ is called a *naive plane*; and if $\omega = |a| + |b| + |c|$, it is a *standard plane*.

The following theorem was proved in (Andres et al. 1997) by employing results from (Veelaert 1993).

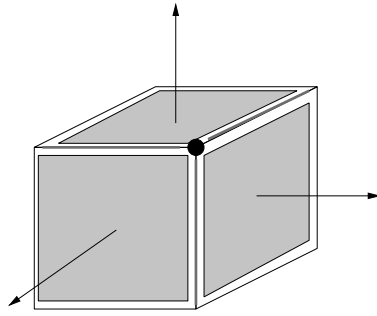


Fig. 3. Example of a tripod associated to a 0-cell.

Theorem 14 (Andres et al. 1997) *Every rational digital plane $I_{\alpha_1, \alpha_2, \beta}$ is a naive plane $D_{a, b, c, \mu, \omega}$ with relatively prime coefficients a, b, c , and vice versa.*

In the rest of this section, we characterize upper or lower frontier planes in the incidence grid model. Assume in the definition of supporting planes that S is a set of cells in the incidence grid \mathbb{C}_3 . Each 0-cell of a 3-cell c is incident with three 2-cells of c (see Figure 3). The (outward pointing) normals to these 2-cells form a *tripod*. There are eight different tripods.

Corollary 15 *The normals of all 2-cells of any upper or lower digital frontier plane belong to the same tripod.*

The *main diagonal* \mathbf{v} of a pair of parallel planes in \mathbb{R}^3 is the diagonal vector in a grid cube that has the greatest dot (i.e., inner) product with the normal \mathbf{n} of the planes (i.e., \mathbf{v} has one of the eight possible directions $(\pm 1, \pm 1, \pm 1)$ and length $\|\mathbf{v}\| = \sqrt{3}$; if there is more than one such a direction, we can choose one of them arbitrarily). The distance between both planes in main diagonal direction is called their *main diagonal distance*.

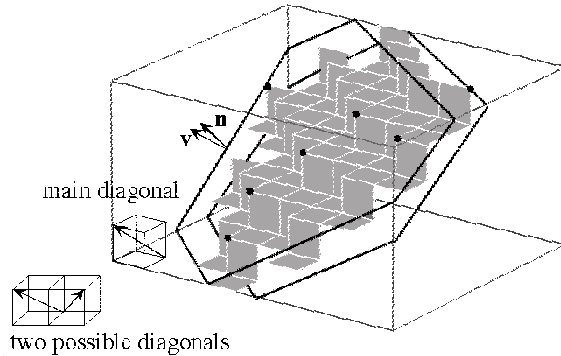


Fig. 4. A DPS of 2-cells; the main diagonal distance between the two parallel planes is less than $\sqrt{3}$ (Klette and Sun 2001).

Recall that in 2D, a 1-path is a 1-DSS (digital straight segment) iff its cells lie between or on a pair of supporting lines whose main diagonal distance is less than $\sqrt{2}$ (see (Rosenfeld and Klette 2001)). Figure 4 shows a DPS of 2-cells; \mathbf{n} is the normal of the shown supporting planes, and \mathbf{v} is the vector in the

main diagonal direction. Note that also allowing a main diagonal distance of “equal to $\sqrt{3}$ ” in the following corollary is of benefit for algorithms.

Corollary 16 *A finite simply 1-connected set of frontier faces of a set of 3-cells is a DPS iff any of its (outward pointing) face normals belongs to one tripod, and the faces lie between or on a pair of parallel Euclidean planes whose main diagonal distance is less than, or equal to $\sqrt{3}$.*

PROOF. Theorem 14 shows that a finite DPS G in the grid-point model is characterized (besides connectivity) by the property that it is between two supporting planes

$$ai + bj + ck = \mu \quad \text{and} \quad ai + bj + ck = \mu + c$$

The upper supporting plane is a translation of the lower supporting plane (by translation vector $(0, 0, 1)$). The main diagonal direction of both (under the assumption $0 < a \leq b \leq c$) is $(-1, -1, +1)$, and the main diagonal distance between both planes is less than, or equal to $\sqrt{3}$.

Now consider a set of 2-cells in the grid-cube model. A translation by $(.5, .5, .5)$ maps all vertices of these 2-cells into grid point positions. The main diagonal distance between two parallel planes is invariant with respect to such a translation. Due to Corollary 15 we also have that all face normals are on a tripod.

For the reverse direction we also apply Theorem 14, and obtain that a main diagonal distance less than $\sqrt{3}$ defines a DPS (or DPS of 2-cells). Now assume that a given finite set G of frontier faces is on or between two parallel planes whose main diagonal distance is equal to $\sqrt{3}$. Then we also have (at least) one 3-cell between both parallel planes (with face normals which do not belong to just one tripod). The additional requests that all face normals belong to one tripod, and that G is simply 1-connected, imply that all 2-cells in G only belong to either the upper or the lower digital frontier plane of one cellular digital plane and are defined on an (even simply-connected) 1-region of 2-cells in $\mathbb{Z}_{x=0}^3$. Altogether, G is a DPS. \square

4 Height and Remainder Maps

From Theorem 14 we know that for any digital plane $I_{\alpha_1, \alpha_2, \beta}$ with rational α_1 and α_2 , there exist relatively prime integers a, b, c and an integer μ such that $I_{\alpha_1, \alpha_2, \beta} = D_{a, b, c, \mu, \max\{|a|, |b|, |c|\}}$; and for any $D_{a, b, c, \mu, \max\{|a|, |b|, |c|\}}$ there exist rational slopes α_1, α_2 and an intercept β such that $D_{a, b, c, \mu, \max\{|a|, |b|, |c|\}} = I_{\alpha_1, \alpha_2, \beta}$.

A naive plane $D = D_{a, b, c, \mu, \omega}$ is *functional* over a coordinate plane, say, xy , if for any pixel (x, y) from xy there is exactly one voxel belonging to D .

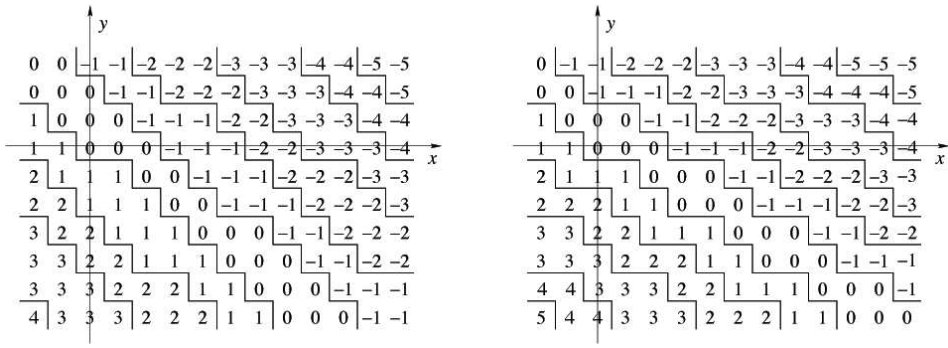


Fig. 5. Two height maps, for $D_{6,7,16,0,16}$ on the left, and $D_{6,9,16,0,16}$ on the right (Brinkov and Barneva 2004).

Without loss of generality, we consider naive planes that are digitizations of Euclidean planes incident with the origin (e.g., by assuming $\mu = 0$). Now assume $0 < a \leq b \leq c$. This condition implies that the naive plane $D_{a,b,c,0,\omega}$ is functional over the plane xy , i.e., each voxel $(x, y, z) \in D_{a,b,c,0,c}$ projects onto a pixel (x, y) in the xy -plane, and for every $(x, y) \in \mathbb{Z}^2$ there is exactly one voxel $(x, y, z) \in D_{a,b,c,0,c}$.

Definition 17 Let $0 < a \leq b \leq c$. The *height map* $M_{a,b,c}^{(h)}$ of $D_{a,b,c,0,\omega}$ is defined on \mathbb{Z}^2 by $M_{a,b,c}^{(h)}(x, y) = \{z \in \mathbb{Z} : (x, y, z) \in D_{a,b,c,0,c}\}$.

Figure 5 illustrates two height maps of naive planes $D_{a,b,c,0,c}$. Let $L_{a,b,c}(z_0) = \{(x, y) \in \mathbb{Z}^2 : (x, y, z_0) \in D_{a,b,c,0,c}\}$, for $z_0 \in \mathbb{Z}$. It follows that $L_{a,b,c}(z_0)$ is an arithmetic line $D(a, b, \mu, \omega)$ with $\mu = -cz_0$ and $\omega = c$; $D(a, b, \mu, \omega)$ is standard if $c = a + b$, “thicker than standard” if $c > a + b$, and “thinner than standard,” but “thicker than naive” if $c < a + b$. The arithmetic lines $L_{a,b,c}(z_0)$, with $z_0 \in \mathbb{Z}$, partition \mathbb{Z}^2 into *equivalence classes* determined by the different values of $M_{a,b,c}^{(h)}$, which are all translation equivalent³ iff a, b are relatively prime (Brinkov and Barneva 2004), see also (Brinkov and Barneva 2003). See Figure 5 on the left for an example with relatively prime integers a, b , and on the right for an example where a, b are not relatively prime. In the former, all equivalence classes are translation equivalent, while in the latter the partition features two different patterns. Any set of $\gcd(a, b) = 3$ consecutive patterns (that are arithmetic lines with arithmetic thickness c) appear periodically in the partition.

Furthermore, $0 < a \leq b \leq c$ implies that the projections $L_{a,b,c}^{(x)}(x_0) = \{(y, z) \in \mathbb{Z}^2 : (x_0, y, z) \in D_{a,b,c,0,c}\}$ and $L_{a,b,c}^{(y)}(y_0) = \{(x, z) \in \mathbb{Z}^2 : (x, y_0, z) \in D_{a,b,c,0,c}\}$, for some $x_0, y_0 \in \mathbb{Z}$, are naive lines with intercept $\mu = -ax_0$ or $\mu = -by_0$, respectively. The arithmetic lines $L_{a,b,c}^{(x)}(x_0)$, for $x_0 \in \mathbb{Z}$, constitute a cover of \mathbb{Z}^2 . The same holds for the arithmetic lines $L_{a,b,c}^{(y)}(y_0)$, for $y_0 \in \mathbb{Z}$; see

³ $A, B \subset \mathbb{Z}^n$ are *translation equivalent* iff there is a translation vector $\mathbf{t} \in \mathbb{Z}^n$ such that $A = \mathbf{t} \oplus B$.

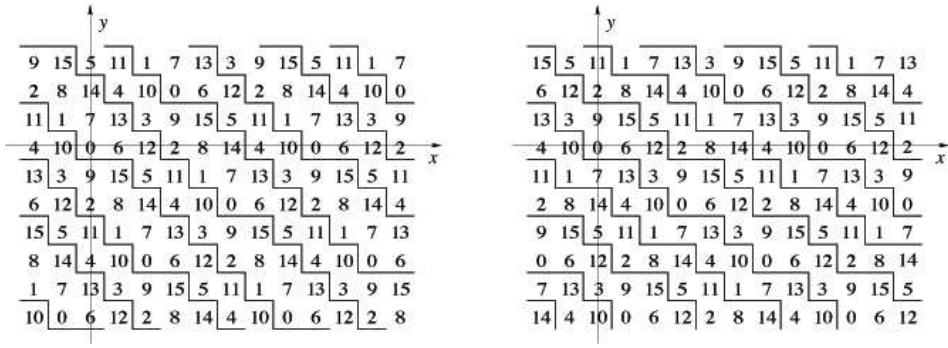


Fig. 6. Two remainder maps for the naive planes shown in Figure 5 (Brimkov and Barneva 2004).

(Debled-Renesson and Reveillès 1994) and (Debled-Renesson 1995).⁴

Naive planes can also be represented by remainders (Debled-Renesson 1995). Let $(x, y, z) \in D_{a,b,c,0,c}$. We assign a value $ax + by + cz$ to the grid point (x, y) , i.e., the remainder modulo c .

Definition 18 Let us consider $0 < a \leq b \leq c$. The *remainder map* $M_{a,b,c}^{(rem)}$ of $D_{a,b,c,0,\omega}$ is defined on \mathbb{Z}^2 by $M_{a,b,c}^{(h)}(x, y) = \{ax + by + cz \pmod{c} : (x, y, z) \in D_{a,b,c,0,c}\}$.

A remainder map is an array that features a partition which has the same *arithmetic line patterns* as those in the partition induced by the height map $M_{a,b,c}^{(h)}$. See Figure 6 for two examples. On the left we have $a = 6$ and $b = 7$, i.e., both integers are relatively prime, which results into remainders in the whole range of $0, \dots, 15$, for $c = 16$. On the right we have $a = 6$ and $b = 9$, i.e., remainders in one equivalence class of the height map are all identical modulo $\gcd(6, 9) = 3$. More in general, we have the following proposition (Brimkov and Barneva 2004).

Proposition 19 Consider the naive plane $D_{a,b,c,0,c} : 0 \leq ax + by + cz < c$, $0 \leq a \leq b \leq c$, and its remainder map $M_{a,b,c}^{(rem)}$.

- 1 Let $\gcd(a, b) = 1$. Then all arithmetic line patterns of the partition of $M_{a,b,c}^{(rem)}$ are equivalent. Each of them involves the numbers $0, 1, 2, \dots, c-1$. See Figure 6a.
- 2 Let $\gcd(a, b) = d \neq 1$. Then the partition of $M_{a,b,c}^{(rem)}$ features two different arithmetic line patterns, as any d consecutive arithmetic lines D_0, D_1, \dots, D_{d-1} appear periodically in the partition. Moreover, for some permutation $(i_0, i_1, \dots, i_{d-1})$ of the indexes $0, 1, \dots, d-1$, for any $k : 0 \leq k \leq d-1$, the line $D_{i_k}, 0 \leq k \leq d-1$ involves only integers in the range $[0, c-1]$ equal to k modulo d . See Figure 6b.

⁴ Using the restriction $\gcd(a, b) = \gcd(a, c) = \gcd(b, c) = 1$; for the general case, see (Brimkov and Barneva 2004).

The equivalent arithmetic lines (i.e., those containing the same values) form an *equivalence class*. Thus we have $\gcd(a, b)$ equivalence classes overall.⁵

Proposition 20 (*Brimkov and Barneva 2004*) $M_{a,b,c}^{(rem)}$, $M_{c-a,b,c}^{(rem)}$, $M_{a,c-b,c}^{(rem)}$, and $M_{c-a,c-b,c}^{(rem)}$, $0 < a \leq b \leq c$, are equivalent to each other either up to a reflection in arbitrary row ($M_{a,b,c}^{(rem)}$ and $M_{a,c-b,c}^{(rem)}$; $M_{c-a,b,c}^{(rem)}$ and $M_{c-a,c-b,c}^{(rem)}$), or up to a reflection in arbitrary column ($M_{a,b,c}^{(rem)}$ and $M_{c-a,b,c}^{(rem)}$; $M_{a,c-b,c}^{(rem)}$ and $M_{c-a,c-b,c}^{(rem)}$), or up to a reflection in arbitrary point, i.e., 180 degree rotation ($M_{a,b,c}^{(rem)}$ and $M_{c-a,c-b,c}^{(rem)}$; $M_{c-a,b,c}^{(rem)}$ and $M_{a,c-b,c}^{(rem)}$).

PROOF. The proof is based on the following two technical lemmas.

Lemma 21 Let $D_{a,b,c,0,c} : 0 \leq ax + by + cz < c$ be a naive plane. Consider its remainder map $M_{a,b,c}^{(rem)}$. Let (x, y) be a point of $M_{a,b,c}^{(rem)}$ with value s , $0 \leq s \leq c - 1$.

- 1 Let the points (x, y) and (x', y') belong to the same equivalence class (digital line) of the related partition, where (x', y') labels one of the following points: $(x, y + 1)$, $(x, y - 1)$, $(x - 1, y)$, $(x + 1, y)$, $(x + 1, y + 1)$, $(x + 1, y - 1)$, $(x - 1, y + 1)$, or $(x - 1, y - 1)$. Then the value of (x', y') is respectively, $s + b$, $s - b$, $s - a$, $s + a$, $s + b + a$, $s - b + a$, $s + b - a$, or $s - b - a$.
- 2 Let now the points (x, y) and (x'', y'') belong to different equivalence classes (digital lines) of the partition, where (x'', y'') labels one of the points: $(x, y + 1)$, $(x, y - 1)$, $(x - 1, y)$, $(x + 1, y)$, $(x + 1, y + 1)$, $(x + 1, y - 1)$, $(x - 1, y + 1)$, or $(x - 1, y - 1)$. Then the value of (x'', y'') is respectively, $s + b - c$, $s - b + c$, $s - a + c$, $s + a - c$, $s + b + a - c$, $s - b + a + c$, $s + b - a - c$, or $s - b - a + c$.

The proof follows immediately from the definition of $M_{a,b,c}^{(rem)}$.

Lemma 22 Consider the digital planes $D_{a,b,c,0,c} : 0 \leq ax + by + cz < c$ and $D_{a,c-b,c,0,c} : 0 \leq ax + (c - b)y + cz < c$ and their remainder maps $M_{a,b,c}^{(rem)}$ and $M_{a,c-b,c}^{(rem)}$, respectively. Let (x, y) be a point of $M_{a,b,c}^{(rem)}$ with a value $v(x, y) = s$, and (x', y') a point of $M_{a,c-b,c}^{(rem)}$ with the same value $v(x', y') = s$. Then (x, y) and $(x, y \pm 1)$ belong to the same equivalence class of $M_{a,b,c}^{(rem)}$ iff (x', y') and $(x', y' \mp 1)$ belong to different equivalence classes of $M_{a,c-b,c}^{(rem)}$.

PROOF. Let (x, y) and $(x, y + 1)$ belong to the same equivalence class of $M_{a,b,c}^{(rem)}$. By Lemma 21, $v(x, y + 1) = s + b < c$, which is equivalent to $v(x', y' -$

⁵ Note that the equivalence relation defined on $M_{a,b,c}^{(rem)}$ is different from the one defined on the height map $M_{a,b,c}^{(h)}$.

$1) = s - (c - b) < 0$, i.e., (x', y') and $(x', y' \mp 1)$ belong to different equivalence classes of $M_{a,c-b,c}^{(rem)}$. Analogously, if (x, y) and $(x, y - 1)$ belong to the same equivalence class of $M_{a,b,c}^{(rem)}$, then $v(x, y - 1) = s - b > 0$, which is equivalent to $v(x', y' + 1) = s + (c - b) > c$, i.e., (x', y') and $(x', y' \pm 1)$ belong to different equivalence classes of $M_{a,c-b,c}^{(rem)}$. \square

After this preparation, consider $M_{a,b,c}^{(rem)}$ and $M_{a,c-b,c}^{(rem)}$. Since $D_{a,b,c,0,c}$ and $D_{a,c-b,c,0,c}$ have the same first and third coefficients, it follows that the corresponding arrays $M_{a,b,c}^{(rem)}$ and $M_{a,c-b,c}^{(rem)}$ are composed by the same set of rows. We will show that they are equivalent up to a reflection in arbitrary row of $M_{a,b,c}^{(rem)}$.

Let (x, y) be an arbitrary point of $M_{a,b,c}^{(rem)}$ with value $v(x, y) = s$. Consider the point $(x, y+1)$. Assume that (x, y) and $(x, y+1)$ belong to the same equivalence class in $M_{a,b,c}^{(rem)}$ (i.e., $s + b < c$). Then by Lemma 21, $v(x, y + 1) = s + b$. Let (x', y') be a point of $M_{a,c-b,c}^{(rem)}$ with the same value $v(x', y') = s$ as (x, y) . Then by Lemma 22, (x', y') and $(x', y' - 1)$ belong to different equivalent classes of $M_{a,c-b,c}^{(rem)}$. Then, again by Lemma 21, $v(x', y' - 1) = s - (c - b) + c = s + b$, i.e., the same as the value $v(x, y + 1)$.

Similarly, consider the point $(x, y - 1)$, and assume that (x, y) and $(x, y - 1)$ belong to the same equivalence class in $M_{a,b,c}^{(rem)}$ (i.e., $s - b > 0$). We have $v(x, y - 1) = s - b$. Then (x', y') and $(x', y' + 1)$ belong to different equivalent classes of $M_{a,c-b,c}^{(rem)}$, and $v(x', y' + 1) = s + (c - b) - c = s - b$, which is the same as the value $v(x, y - 1)$.

The case when (x, y) and $(x, y + 1)$ (resp. (x, y) and $(x, y - 1)$) belong to different equivalence classes can be handled analogously. Thus we can conclude that the array $M_{a,c-b,c}^{(rem)}$ can be obtained from the array $M_{a,b,c}^{(rem)}$ by reflection in arbitrary row of $M_{a,b,c}^{(rem)}$. See Figure 6.

In an analogous way it follows that $M_{a,b,c}^{(rem)}$ and $M_{c-a,b,c}^{(rem)}$ are equivalent up to a reflection in arbitrary column of $M_{a,b,c}^{(rem)}$. The other equivalences can be obtained in a similar fashion, taking advantage of those already proved. For instance, we can now apply the last fact above to $M_{a,c-b,c}^{(rem)}$ and obtain that $M_{c-a,c-b,c}^{(rem)}$ and $M_{a,c-b,c}^{(rem)}$ are equivalent up to a reflection in arbitrary column. Hence, $M_{c-a,c-b,c}^{(rem)}$ can be obtained from $M_{a,b,c}^{(rem)}$ by a reflection in arbitrary row followed by a reflection in arbitrary column, i.e., by a reflection in arbitrary point of $M_{a,b,c}^{(rem)}$. \square

This is called the *Symmetry Lemma* in (Brimkov and Barneva 2004), which defines a special type of symmetry between naive planes $D_{a,b,c,0,c}$, $D_{c-a,b,c,0,c}$, $D_{a,c-b,c,0,c}$, and $D_{c-a,c-b,c,0,c}$. If one or both parameters a and b are larger than

$c/2$, then the Symmetry Lemma allows to consider w.l.o.g. *symmetric naive planes* $D_{a,c-b,c,0,c}$ or $D_{c-a,c-b,c,0,c}$ where the two first parameters do not exceed $c/2$ (see Figure 6). This may be useful for studying the connectivity number of a digital plane (see Section 6).

5 Periodicity

We start by introducing various notions related to the subject of this section.

A *position* (i, j) in an array $X = (X(i, j))_{0 \leq i, 0 \leq j}$ is defined by a row i and a column j ; $X(i, j)$ is the *element* of X at position (i, j) . The elements of X are letters in an alphabet A .

Let $S \subseteq \mathbb{Z}^2 = \{(i, j) \in \mathbb{Z}^2 : i, j \geq 0\}$. The restriction $X[S]$ of X to positions in S is called a *factor of X on S* . If $S = \mathbb{Z}^2$ or $S = \mathbb{Z}_+^2$, we will write X instead of $X[S]$, for short.

Definition 23 A nonzero vector \mathbf{v} in \mathbb{Z}^2 is called a *symmetry vector* for $X[S]$ iff $X(i, j) = X(\mathbf{v} + (i, j))$ for all $(i, j) \in S$ such that $\mathbf{v} + (i, j) \in S$. \mathbf{v} is called a *periodicity vector* or a *period* for $X[S]$ iff for any integer k the vector $k\mathbf{v}$ is a symmetry vector for $X[S]$.

An infinite array X on \mathbb{Z}_+^2 is called *2D-periodic* iff there are two linearly independent vectors \mathbf{u} and \mathbf{v} in \mathbb{Z}^2 such that $\mathbf{w} = i\mathbf{u} + j\mathbf{v}$ is a period for X for any $(i, j) \in \mathbb{Z}^2$ and $\mathbf{w} \in \mathbb{Z}_+^2$. X is called *1D-periodic* iff all periods of X are parallel vectors. If X has no period, it is *aperiodic*.

Periodicity of a 3D set $X[S]$ where $S \subseteq \mathbb{Z}^3$ is defined analogously.

Let X be a 2D-periodic infinite array on \mathbb{Z}_+^2 . The set of symmetry vectors of X defines (by additive closure) a sub-lattice Λ of \mathbb{Z}^2 . Any basis of Λ is a *basis* of X .

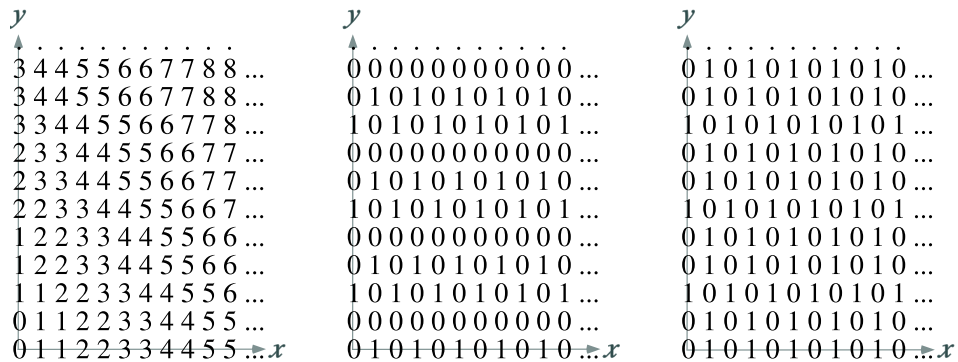


Fig. 7. (Brinkov 2002) Left: $I_{\frac{1}{2}, \frac{1}{3}, 0}^{(m, n)}$. Middle: $i_{\frac{1}{2}, \frac{1}{3}, 0}^{(r)}(m, n)$. Right: $i_{\frac{1}{2}, \frac{1}{3}, 0}^{(c)}(m, n)$.

In analogy with the chain codes for digital curves (Freeman 1961), and following (Brimkov and Barneva 2005), below we define *step codes*. These appear to be a convenient technical tool for studying the structure of digital objects (in particular digital lines and planes) since they are defined on alphabets with a small number of letters (usually binary or ternary).

We start with $i_{\alpha_1, \alpha_2, \beta}(0, 0) = I_{0,0} \in \{0, 1\}$. Then we define:

$$i_{\alpha_1, \alpha_2, \beta}(0, n+1) = I_{0, n+1} - I_{0, n} = \begin{cases} 0 & \text{if } I_{0, n+1} = I_{0, n} \\ 1 & \text{if } I_{0, n+1} = I_{0, n} + 1 \end{cases} \quad \text{for } n \geq 0$$

$$i_{\alpha_1, \alpha_2, \beta}(m+1, 0) = I_{m+1, 0} - I_{m, 0} = \begin{cases} 0 & \text{if } I_{m+1, 0} = I_{m, 0} \\ 1 & \text{if } I_{m+1, 0} = I_{m, 0} + 1 \end{cases} \quad \text{for } m \geq 0$$

In addition to these “initial values,” we also define row-wise step codes

$$i_{\alpha_1, \alpha_2, \beta}^{(c)}(m, n+1) = I_{m, n+1} - I_{m, n} = \begin{cases} 0 & \text{if } I_{m, n+1} = I_{m, n} \\ 1 & \text{if } I_{m, n+1} = I_{m, n} + 1 \end{cases} \quad \text{for } m \geq 1$$

and column-wise step codes

$$i_{\alpha_1, \alpha_2, \beta}^{(r)}(m+1, n) = I_{m+1, n} - I_{m, n} = \begin{cases} 0 & \text{if } I_{m+1, n} = I_{m, n} \\ 1 & \text{if } I_{m+1, n} = I_{m, n} + 1 \end{cases} \quad \text{for } n \geq 1$$

Values in the 0th row and 0th column are used in both the column-wise and row-wise step codes; see Figure 7. Assumptions $0 \leq \alpha_1 \leq 1$ and $0 \leq \alpha_2 \leq 1$ guarantee that codes 0 and 1 are sufficient, i.e., the step codes are 2D arrays on a binary alphabet $A = \{0, 1\}$. Since row-wise and column-wise step codes exhibit analogous properties, (as demonstrated in (Brimkov and Barneva 2005), see also (Brimkov 2002)), we will only use row-wise step codes in the sequel, and will omit the superscript (r) .

Definition 24 (Brimkov and Barneva 2005) $i_{\alpha_1, \alpha_2, \beta} = \{(m, n, i_{\alpha_1, \alpha_2, \beta}(m, n)) : m, n \in \mathbb{Z}, m, n \geq 0\}$ is a *step code of a digital plane quadrant*, or, for short, a *quadrant step code*, with slopes α_1 and α_2 and intercept β .

If we do not require m, n to be nonnegative, we obtain a *step code of a digital plane*. For short, we call it a *plane step code*.

Digital planes and plane quadrants have analogous properties, as plane and quadrant step codes do. To simplify our notation, we will use $I_{\alpha_1, \alpha_2, \beta}$ to denote

both digital planes and plane quadrants, and $i_{\alpha_1, \alpha_2, \beta}$ for plane or quadrant step codes.

For $D \subseteq \mathbb{R}^2$, let

$$i_{\alpha_1, \alpha_2, \beta}^D = \{(m, n, i_{\alpha_1, \alpha_2, \beta}(m, n)) : (m, n) \in D \cap \mathbb{Z}^2\}$$

If α_1 or α_2 is irrational, then we speak about an *irrational plane step code*; otherwise it is a *rational plane step code*.

(Lunnon and Pleasants 1992) show that rational digital straight lines are translation equivalent if they have identical slopes. Rational digital planes with identical slopes are also translation equivalent, see (Brimkov and Barneva 2004). This implies that translation invariant properties of rational digital planes are independent of intercepts; the translation equivalence classes of all rational digital planes can be uniquely identified by $I_{\alpha_1, \alpha_2, \beta}$ or $i_{\alpha_1, \alpha_2, \beta}$. Note however that the above properties do not apply to the case of irrational digital planes, as follows, e.g., from considerations in (Brimkov and Barneva 2005).

It is well known that chain codes of rational digital rays/lines (that are digitizations of rays/lines with rational coefficients, see (Rosenfeld and Klette 2001)) are periodic while those of irrational digital rays/lines are aperiodic (Brons 1974). Below we study periodicity of quadrant step codes. We consider quadrant step codes rather than plane step codes for the sake of technical convenience. Since a plane quadrant is a 2D counterpart of a ray, this way we also parallel the one-dimensional considerations that are usually in terms of digital rays.

Theorem 25 *Any rational quadrant step code is 2D-periodic. Any irrational quadrant step code is either 1D-periodic or aperiodic.*

The formal proof of this statement is too lengthy to be included in the present survey (see (Brimkov and Barneva 2005)). It particularly relies on the following well-known fact: For any rational Euclidean plane P there are (infinitely many) pairs of linearly independent *rational directions* (i.e., vectors with rational coordinates that are collinear with P). In this case the corresponding digital plane quadrant and its step code are 2D-periodic. For any irrational Euclidean plane P one of the following conditions is met. (i) P has no rational direction, i.e., there is no rational vector that is parallel to P . Note that in this case P may either contain no integer or rational points, or may contain a single point of this kind. (ii) P has a rational direction. In this case P either contains infinitely many equidistant integer points lying on a line, or P is parallel to such a line. One can show that in Case (i) the digital plane quadrant of P is aperiodic, while in Case (ii) it is 1D-periodic. The same applies to the corresponding quadrant step codes.

Next we obtain another property related to rational digital planes and their step codes. W.l.o.g., consider a rational plane through the origin $P : ax +$

$by + cz = 0$, the corresponding digital plane $D_{a,b,c,0,c}$, and its plane step code $i_{\alpha_1, \alpha_2, \beta}$. Let Λ be the integer lattice in P , B a basis for Λ , and Λ' and B' the orthogonal projections of Λ and B over the xy -plane, respectively. Then Λ' is a sub-lattice of \mathbb{Z}^2 and B' a basis for Λ' . With this denotations we can state the following theorem.

Theorem 26 (*Brimkov and Barneva 2005*) *Given a rational plane $P : ax + by + cz = 0$, let Λ be the integer lattice in P and Λ' its orthogonal projection over the xy -plane. Then for any basis for Λ' , the lattice cells of Λ' have constant area $\max\{|a|, |b|, |c|\}$.*

PROOF. W.l.o.g., let $0 \leq a \leq b \leq c$, i.e., $c = \max\{a, b, c\}$. It is well-known that, given two simple polygons⁶ in P with equal area, their orthogonal projections over the coordinate xy -plane have the same area, as well. It is also a well-known fact that all bases of the integer lattice Λ in P generate cells with equal area. Hence, it is enough to estimate the area of a parallelogram that is the orthogonal projection of a cell determined by an arbitrary basis of Λ . As a first basis vector one can chose $u = (0, c/\gcd(b, c), -b/\gcd(b, c))$. Then as a second basis vector one can chose $v = (\gcd(b, c), y^*, z^*)$, where y^*, z^* form a solution of the linear Diophantine equation $a \cdot \gcd(b, c) + by + cz = 0$, and y^* is the minimal positive integer with this property. The special construction of u and v (and, especially, the minimality of y^*) assures that these two vectors indeed form a basis for Λ . Then the orthogonal projections of u and v over the xy -plane are respectively the vectors $u' = (0, c/\gcd(b, c))$ and $v' = (\gcd(b, c), y^*)$, which form a basis for the lattice Λ' related to the plane step code. Then the area of the corresponding cell generated by u' and v' equals $|\det(u'|v')| = c = \max\{a, b, c\}$. \square

We say that an infinite array X on \mathbb{Z}_+^2 is *tiled* by a (finite) rectangular factor W if X is a pairwise disjoint repetition of W . Rectangular tilings are of interest because of their simple special shape. It can be shown that any 2D-periodic array on \mathbb{Z}_+^2 can be tiled by a rectangular tile (see, e.g., (Brimkov 2000)). This implies that any rational quadrant step code can be tiled by a rectangular tile of a certain size.

Let X be an array on \mathbb{Z}_+^2 . An $m \times n$ rectangle $S \subset \mathbb{Z}_+^2$ defines an $m \times n$ -factor of X . Given two integers $k, l \geq 0$, we call a (k, l) -*suffix* of X the sub-array of X determined by its rows and columns with indexes greater than or equal to k and l , respectively. Digital 2D ray X is called *ultimately periodic* if there are integers $k, l \geq 0$ such that the (k, l) -suffix of X has a period vector. X is *uniformly recurrent* if for every integer $n > 0$ there is an integer $N > 0$ such that every square factor of size $N \times N$ contains every square factor of size $n \times n$.

⁶ A polygon is simple iff it is homeomorphic to a disc.

Let $P_X(m, n)$ be the number of $m \times n$ -factors of X . For example, $P_X(0, 0) = 1$ for any X and $P_X(1, 1)$ is the number of distinct letters in X . We consider binary words on the alphabet $A = \{0, 1\}$. P_X generalizes the complexity function $P(w, n)$ defined (e.g.) in (Allouche and Shallit) for 1D words w . Recall that the *complexity function* $P_w(n)$ of such a word w is defined as the number of different n -factors of w . A binary word w with $P_w(n) \leq n$ for some n , is (ultimately) periodic. Sturmian words are the words that have lowest complexity among the non-ultimately periodic words, i.e., of complexity $P_w(n) = n + 1$ for any $n \geq 0$. It is also well-known that any Sturmian word is a chain code of an irrational straight line and is uniformly recurrent. In higher dimensions the situation is more complicated. For instance, it is still unknown whether a notion of minimal complexity can be reasonably defined (see (Berthé and Vuillon 2000a) and the discussion therein). To a certain extent the same applies to the notion of 2D Sturmian word. Initially it has been expected that 2D words of minimal complexity are step codes⁷ of irrational planes with no rational direction. Such words were believed to have complexity $mn + 1$. However, it has been recently shown that a 2D word of complexity $mn + 1$ cannot be uniformly recurrent and does not appear to be a step code of any plane (Cassaigne 1999). Therefore, it makes sense to call 2D Sturmian words the ones that appear to be step codes of irrational planes which do not have a rational direction. Such kind of words obtained within a number of diverse digitization schemes have been investigated by S. Ito, M. Ohtsuki, L. Vuillon, V. Berthé, R. Tijdeman among others. See, e.g. (Vuillon 1998), (Arnoux et al. 2001), (Berthé and Vuillon 2000a), (Berthé and Vuillon 2000b), (Cassaigne 1999), (Ito and Ohtsuki 1994), (Berthé and Vuillon 2001) for recent contributions. Here we present some results in the context of the plane step codes.

An aperiodic irrational plane step code X still possesses certain “quasiperiodicity” (uniform recurrence). Thus every rectangular block appearing in X , appears in it infinitely many times and with bounded gaps. Moreover, all step codes of irrational planes with the same coefficients contain the same set of rectangular factors, and any rectangular factor of an irrational plane step code is also a factor of a rational plane step code. We also have that if X is an irrational plane step code, then $P_X(m, n)$ is unbounded. For the above and other results see (Brimkov 2002) and (Brimkov and Barneva 2005).

An important array characteristic is its balance. Let $h(U)$ denote the number of 1’s in a binary array U . Given two binary arrays U and V of the same size $m \times n$, $\delta(U, V) = |h(U) - h(V)|$ is their *balance*. A set X of arrays is said to be α -balanced for a certain *constant* $\alpha > 0$, if $\delta(U, V) \leq \alpha$ for all pairs of $(m \times n)$ -arrays $U, V \in X$, where m and n are arbitrary positive integers. An infinite array A is said to be α -balanced if its set of factors is α -balanced. Array balances are familiar from studies in number theory, er-

⁷ Step-codes of digital planes have been defined in certain ways, not necessarily the same as the one used in this paper, but, as a matter of fact, equivalent to it in terms of basic properties. See, for instance, (Berthé and Vuillon 2000a).

godic theory, and theoretical computer science. For a recent study on balance properties of multidimensional words on two or three letter alphabets see, e.g., (Berthé and Tijdeman 2002). One can show that if X is a row-wise plane step code, then $\delta(U, V) \leq m$ for any pair of $(m \times n)$ -factors of X , $m, n \geq 0$ (Brimkov and Barneva 2005). This bound is reachable, hence the step codes of digital planes are, overall, non-balanced (Brimkov and Barneva 2005).

Before presenting some other results, we provide a brief discussion on the structure of a digital plane quadrant. Recall that an (m, n) -window at a point $(p, q) \in \mathbb{Z}^2$ is a set of points $(i, j) \in \mathbb{Z}^2$ with $p \leq i < p + m$ and $q \leq j < q + n$. An (m, n) -cube at a point $(i, j) \in \mathbb{Z}^2$ of a digital plane P is the set $\{(x, y, z) \in P : i \leq x \leq i + m - 1 \text{ and } j \leq y \leq j + n - 1\}$. Two (m, n) -cubes at two different points (i, j) and (i', j') of a digital plane are geometrically equivalent if each of them can be obtained from the other by an appropriate translation. By $C_X(m, n)$ we denote the number of different (m, n) -cubes over the points of a digital plane X . $C_X(m, n)$ is an important parameter characterizing a digital plane structure (see, e.g., (Reveillès 1995)) and is closely related to the complexity function of a plane step code. The following properties have been proved in (Brimkov and Barneva 2005). It follows that $C_X(m, n) \leq mn$. If X is rational, then $C_X(m, n) \leq lcm(q_1, q_2)$, where q_1 and q_2 are the denominators of the coefficients of x_1 and x_2 in the analytical plane representation. We always have $P_X(m, n) \geq C_X(m, n)$. If X is irrational and aperiodic, then $P_X(m, n) \geq mn$.

We conclude this section by listing some results related to a conjecture by M. Nivat about periodicity of infinite binary 2D words. He conjectured that if for some integers $m, n \geq 0$ an infinite bi-dimensional 0/1 array A has complexity $P_A(m, n) \leq mn$, then A has at least one period vector (Nivat 1997). Note that the converse is not true, in general: an array may be 1D-periodic but its complexity may be higher than mn (see (Berthé and Vuillon 2000a)). Only partial results for small values of m and n have been proved regarding this conjecture. In (Epifanio et al. 2003) a weaker statement is proved under the condition $P_A(m, n) \leq \frac{1}{100}mn$. This result was recently improved by reducing the constant factor $\frac{1}{100}$ to $\frac{1}{12}$ (Quas and Zamponi 2004). For the special case of arrays that are plane step codes, we have the following results (Brimkov and Barneva 2005).

Theorem 27 *Let i_X be a quadrant step code of a digital plane X . i_X has a period vector if and only if for some integers $m, n \geq 0$, $P_{i_X}(m, n) < mn$.*

If for some $m, n \geq 0$ an equality $P_{i_X}(m, n) = mn$ holds, it seems to imply the condition $P_{i_X}(m, n + 1) < m(n + 1)$, under which Theorem 27 applies. To prove this remains as a further task.

Next we present an asymptotic result in terms of $C_R(m, n)$. As already mentioned, Definition 23 straightforwardly extends to one for periodicity of a 3D set $X[S]$ where $S \subseteq \mathbb{Z}^3$. We have the following theorem.

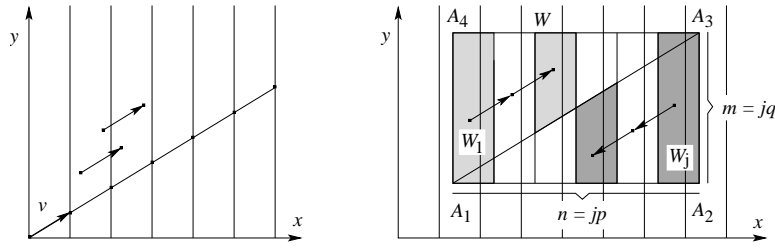


Fig. 8. Illustration to the proof of Theorem 28.

Theorem 28 *Let R be a Euclidean plane quadrant and I_R the corresponding digital plane quadrant. Then I_R has at least a 1D-period if and only if*

$$\lim_{m,n \rightarrow \infty} \frac{C_R(m,n)}{mn} = 0$$

PROOF. Let first assume that $\lim_{m,n \rightarrow \infty} \frac{C_R(m,n)}{mn} = 0$. Then there exist positive integers m_0, n_0 such that for any pair of integers m, n with $m \geq m_0$ and $n \geq n_0$, we have $\frac{C_R(m,n)}{mn} < \frac{1}{2}$, i.e.,

$$C_R(m,n) < \frac{1}{2}mn \quad (5)$$

Obviously, $C_R(m,n) \leq P_R(m,n)$. It is not hard to realize that we also have $P_R(m,n) \leq 2C_R(m,n)$. To see this, let i_R be the step code of R and let us define an (m,n) -window of i_R at a point (i,j) to be the $m \times n$ binary array $\{i_R(x,y) : i \leq x \leq i+m-1, j \leq y \leq j+n-1\} \subset i_R$. Now, let Q and Q' be two geometrically equivalent (m,n) -cubes and H and H' the corresponding (m,n) -windows of i_R at points (i,j) and (i',j') , respectively. Since Q and Q' are geometrically equivalent, if $i_R(i,j) = i_R(i',j')$ then H and H' are equivalent 0/1 arrays, otherwise they are different. Moreover, the value $i_R(i,j)$ (resp. $i_R(i',j')$), that is either 0 or 1, completely and uniquely determines H (resp. H'). Thus we have that there may be at most two different (m,n) -windows of i_R that correspond to geometrically equivalent (m,n) -cubes. Hence, $P_R(m,n) \leq 2C_R(m,n)$. Then (5) implies that for enough large m and n we have $C_R(m,n) < 2 \cdot (\frac{1}{2}mn) = mn$. Then, by Theorem 27 we obtain that the quadrant step code i_R corresponding to R has a period vector. Clearly, I_R will have a period vector as well.

Now let $v = (p, q, r)$, $p \geq q$, be a period vector for I_R , where p, q and r are fixed integers. Let $v' = (p, q)$ be its projection on the coordinate xy -plane. Because of the symmetry of the discrete space, we can assume without loss of generality that R makes with the xy -plane an angle θ with $0 \leq \theta \leq \arctan \sqrt{2}$. Then there is a one-to-one correspondence between the voxels of I_R and the points of \mathbb{Z}_+^2 . So to obtain quantitative estimations, one can work with projections of (m,n) -cubes over the xy -plane rather than with the (m,n) -cubes themselves. Consider the set of nonnegative integer points of the form $u^{(i)} = i \cdot v' = (ip, iq)$ for $i = 0, \pm 1, \pm 2, \dots$. They are projections on the xy -plane of points of I_R ,

generated by the period v . The points $u^{(i)}$ belong to a line determined by v' and induce a partition of \mathbb{Z}_+^2 into a set S of vertical strips delimited by the vertical rays $x = ip$, $y \geq 0$, for $i = 0, \pm 1, \pm 2, \dots$ (Figure 8 (*Left*)). Since v is a symmetry vector of I_R , any two strips from S correspond to regions of i_R that are equivalent up to translation by vector v .

Now consider an (m, n) -window $W = A_1A_2A_3A_4$ of \mathbb{Z}_+^2 with $m = jp$ and $n = jq$ (see Figure 8 (*Right*)). It corresponds to an (m, n) -cube C of I_R . Partition W into j rectangles W_t ($t = 1, 2, \dots, j$) of width p and height jq and consider their pre-images C_t ($t = 1, 2, \dots, j$) from I_R under the orthogonal projection onto the xy -plane. We notice with the help of Figure 8 (*Right*) that the set of voxels from C_1 corresponding to W_1 completely determines (through translation by the vector v) all the other C_t 's portions that correspond to W_t 's portions over the diagonal A_1A_3 . Similarly, the set of voxels from C_j corresponding to W_j completely determines (through translation by vector $(-v)$) all the other C_t 's portions that correspond to W_t 's portions below the diagonal A_1A_3 . Thus the sets of voxels from C_1 and C_j are sufficient to completely recover the whole (m, n) -cube C . Because of the one-to-one correspondence between voxels from I_R and elements of \mathbb{Z}_+^2 , the number of voxels in a set C_t equals the number of integer points in a strip W_t , so C_1 and C_j contain overall $2(p \cdot jq)$ voxels. From this last fact and taking advantage of the above-mentioned inequality $C_R(m, n) \leq mn$, one can easily obtain that vertical perturbations of the plane R through the window W can induce no more than $2(p \cdot jq)$ different (m, n) -cubes. Then for the ratio of $C_R(m, n)$ and mn we have the upper bound

$$\frac{C_R(m, n)}{mn} \leq \frac{2pjq}{j^2pq} = \frac{2}{j} = \frac{2p}{n}$$

which approaches 0 as n approaches infinity. \square

6 Connectivity

We defined α -connected sets in Section 1. In the rest of this section, for the sake of certain technical convenience, we adopt the terminology within the grid-cell model. All definitions and results can immediately be translated into grid-point model terms by substituting 0/1 by 8/4 (in 2D) and 0/1/2 by 26/18/6 (in 3D). We investigate digital plane connectivity in terms of the analytical Definition 13.

Definition 29 An arithmetic line/plane D ($D = D_{a,b,\mu,\omega}$ if D is an arithmetic line and $D = D_{a,b,c,\mu,\omega}$ if D is an arithmetic plane) is called α -separating in \mathbb{Z}^n ($n = 2, 3$) iff $\mathbb{Z}^n \setminus D$ is not α -connected ($0 \leq \alpha \leq n - 1$).

If $\mathbb{Z}^n \setminus D$ is $(n - 1)$ -connected, then D is said to have $(n - 1)$ -gaps.

If D is α -separating ($1 \leq \alpha \leq n - 1$) but not β -separating ($0 \leq \beta \leq \alpha - 1$) in

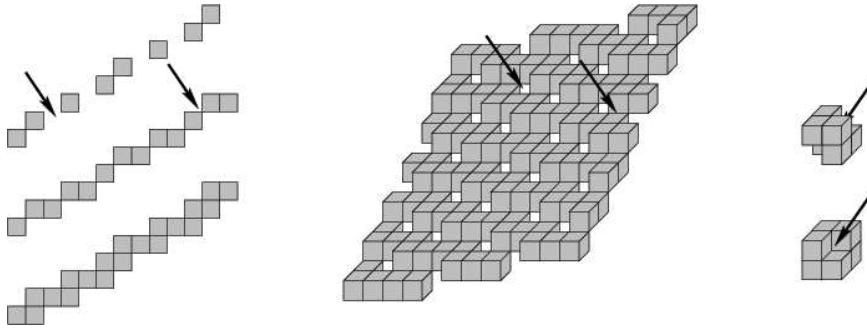


Fig. 9. *Left:* From top to bottom: portions of arithmetic lines defined by $0 \leq 3x - 5y < 3$, $0 \leq 3x - 5y < 5$ (naive line), and $0 \leq 3x - 5y < 8$ (standard line). The first one has 1-gaps (and, therefore, also 0-gaps; a 1-gap is pointed out by an arrow), the second one has 0-gaps (one of them pointed out by an arrow) but no 1-gaps, and the third one is gap-free. *Middle:* Portion of an arithmetic plane defined by $0 \leq 2x + 5y + 9z < 7$. It has 2-gaps (and, therefore, also 1- and 0-gaps). A 2-gap and a 1-gap are pointed out by arrows. *Right:* Configuration of voxels (in two different orientations) that features a 0-gap (pointed out by an arrow). According to Theorem 30, an arithmetic plane with coefficients 2, 5, and 9 has 0-gaps but no 1- or 2-gaps if and only if its thickness ω satisfies $a_2 + a_3 = 14 \leq \omega < a_1 + a_2 + a_3 = 16$.

\mathbb{Z}^n , then D has β -gaps.

It is well-known that an arithmetic line $D_{a,b,\mu,\omega}$ becomes 0-disconnected iff $\omega < \max\{|a|, |b|\}$. Similarly, an arithmetic plane $D_{a,b,c,\mu,\omega}$ no longer has grid points on all the vertical grid lines iff $\omega < \max\{|a|, |b|, |c|\}$ (Reveillès 1991).

Figure 9 illustrates gaps. An arithmetic line is gapfree (which is equivalent to 0-gapfree) iff it is 1-connected; and it is 1-gapfree iff it is 0-connected. A naive line is 0-connected and 1-separating in \mathbb{Z}^2 , and a standard line is 1-connected and 0-separating in \mathbb{Z}^2 . Consider arithmetic lines $D_{a,b,\mu,\omega} = \{(i, j) \in \mathbb{Z}^2 : \mu \leq ai + bj < \mu + \omega\}$, for relatively prime integers a, b with $0 \leq a \leq b$, and integers $\omega \geq 0, \mu$. We have

- (i) D is 0-disconnected iff $\omega < b$ (i.e., D has 1-gaps, see Definition 29).
- (ii) D is 0-connected and has 0-gaps iff $b \leq \omega < a + b$.
- (iii) D is 1-connected and gapfree iff $a + b \leq \omega$.

The above properties have been studied, for example., in (Reveillès 1991), (Andres et al. 1997), (Debled-Renesson 1995).

A standard arithmetic plane is 0-separating and gapfree; it has no 2-, 1-, or 0-gaps. A naive arithmetic plane is 2-separating but not necessarily 1- or 0-separating; it can have 1- or 0-gaps.

Theorem 30 (Andres et al. 1997) *Let $D_{a_1, a_2, a_3, \mu, \omega}$ be an arithmetic plane, where a_1, a_2, a_3 are relatively prime integers with $0 \leq a_1 \leq a_2 \leq a_3$ and $\omega \geq 0$. Then if $\omega < a_3$, the plane has 2-gaps; if $a_3 \leq \omega < a_2 + a_3$, it has 1-gaps and is 2-separating in \mathbb{Z}^3 ; if $a_2 + a_3 \leq \omega < a_1 + a_2 + a_3$, it has 0-gaps and is*

1-separating in \mathbb{Z}^3 ; and if $a_1 + a_2 + a_3 \leq \omega$, it is 0-gapfree.

PROOF. For a given digital plane $D_{a_1, a_2, a_3, \mu, \omega}$, we define its *control value* at the integer point $x = (x_1, x_2, x_3)$ as $\Pi(x, D_{a_1, a_2, a_3, \mu, \omega}) = \mu + a_1x_1 + a_2x_2 + a_3x_3$. The following is a well-known fact:

Fact 31 (Reveillès 1991) *An arithmetic plane $D_{a_1, a_2, a_3, \mu, \omega}$ has k gaps iff there are two k -adjacent voxels $p = (p_1, p_2, p_3)$ and $q = (q_1, q_2, q_3)$ for which $\Pi(p, D_{a_1, a_2, a_3, \mu, \omega}) < 0$ and $\Pi(q, D_{a_1, a_2, a_3, \mu, \omega}) \geq 0$.*

Since all rational digital planes are translation equivalent, w.l.o.g. we may assume that $\mu = 0$. We want to show that $\omega = \sum_{i=k+1}^n a_i$, where $n = 3$ and $k = 2$ or 3 , is the least value for which $D_{a_1, a_2, a_3, \mu, \omega}$ has no k -gaps. First we show that there is at least one k -gap for $\omega = \sum_{i=k+1}^n a_i - 1$. Since $\gcd(a_1, a_2, a_3) = 1$, there is $y = (y_1, y_2, y_3) \in \mathbb{Z}^3$, such that $a_1y_1 + a_2y_2 + a_3y_3 = -1$. Consider the integer point $p = (p_1, p_2, p_3)$ with $p_i = y_i$, $i = 1, 2, 3$. We have $\Pi(p, D_{a_1, a_2, a_3, \mu, \omega}) = -1$. Now consider the integer point $q = (q_1, q_2, q_3)$ with $q_i = p_i$ for $1 \leq i \leq k$ and $q_i = p_i + 1$ for $k + 1 \leq i \leq n$. By construction, p and q are k -neighbors. We have $\Pi(q, D_{a_1, a_2, a_3, \mu, \omega}) = \sum_{i=1}^n a_i q_i = \sum_{i=1}^n a_i p_i + \sum_{i=k+1}^n a_i = -1 + \sum_{i=k+1}^n a_i = \omega \geq 0$. Hence, by Fact 31, a plane with thickness $\omega = \sum_{i=k+1}^n a_i - 1$ has k -gaps.

Now we show that if $\omega = \sum_{i=k+1}^n a_i$, then $D_{a_1, a_2, a_3, \mu, \omega}$ has no k -gap. Consider two integer points $p = (p_1, p_2, p_3)$ and $q = (q_1, q_2, q_3)$ such that $\Pi(p, D_{a_1, a_2, a_3, \mu, \omega}) = -1$ and q is a k -neighbor of p . The latter means that $q_i = p_i + e_i$, where $|e_i| \leq 1$ and $\sum_{i=1}^n |e_i| \leq n - k$. Then $\Pi(q, D_{a_1, a_2, a_3, \mu, \omega}) = \sum_{i=1}^n a_i p_i + \sum_{i=1}^n a_i e_i \leq -1 + \sum_{i=k+1}^n a_i$, i.e., $\Pi(q, D_{a_1, a_2, a_3, \mu, \omega}) \leq \omega - 1$. Hence q cannot be on the same side of $D_{a_1, a_2, a_3, \mu, \omega}$ as p and, therefore, $D_{a_1, a_2, a_3, \mu, \omega}$ has no k -gap. \square

Clearly, the above proof applies also to arbitrary dimensions n .

(Reveillès 1991) stated for arithmetic lines equivalences between 0-gapfreeness and 1-connectedness, and 1-gapfreeness and 0-connectedness. This cannot be repeated for arithmetic planes. For rational digital planes connectivity is a translation-invariant property. W.l.o.g. we consider grid-line intersection digitizations of rational planes $ax + by + cz = 0$ which are incident with the origin, and $D_{a, b, c, 0, \omega}$ is the corresponding arithmetic plane with thickness $\omega \in \mathbb{Z}_+$ and $a, b, c \in \mathbb{Z}_+$ with $\gcd(a, b, c) = 1$.

Definition 32 For $\alpha = 2, 1, 0$ and $a, b, c \in \mathbb{Z}_+$, let

$$\Omega_\alpha(a, b, c) = \max\{\omega : D_{a, b, c, 0, \omega} \text{ is } \alpha\text{-disconnected}\}$$

be the α -connectivity number of the class of all arithmetic planes $D_{a, b, c, \omega}$, with $\omega \in \mathbb{Z}_+$.

In other words, $\omega = \Omega_\alpha(a, b, c) + 1$ is the smallest integer such that $D_{a,b,c,0,\omega}$ is α -connected. Evidently, $\Omega_\alpha(a, b, c) \leq \Omega_\beta(a, b, c)$ if $\alpha \geq \beta$, with $\alpha, \beta \in \{2, 1, 0\}$. Naive planes are always 0-connected, i.e., $\Omega_0(a, b, c) \leq \max\{a, b, c\}$, and standard planes are always 2-connected, i.e., $\Omega_2(a, b, c) \leq a + b + c$. Connectivity numbers remain constant when permuting a, b, c , e.g., $\Omega_\alpha(a, b, c) = \Omega_\alpha(b, c, a)$.

A pair of voxels $p = (i, j, k)$ and $q = (i + 1, j + 1, k + 2)$ (see Figure 10 (*Left*)) defines a *jump*. A naive plane $D_{a,b,c,\mu,c}$ (with $c = \max\{a, b, c\}$) contains a jump iff $c < a + b$ (Brimkov and Barneva 2002). This last result has been used in the design of an efficient algorithm for obtaining 2-gap-free digitizations of polyhedral surfaces. Existence of jumps in a digital plane may lead to a situation as the one illustrated in Figure 10 (*Right*). It shows a naive plane where 0-connected sets of pixels in the height map may be projections of 0-disconnected sets of voxels in the naive plane. The Symmetry Lemma (Proposition 20) allows to transform such naive planes into symmetric (in the sense of the Symmetry Lemma) naive planes where $c < a + b$ is not true anymore. This also allows to conclude:

Proposition 33 $\Omega_0(a, b, c) = \Omega_0(c - a, b, c) = \Omega_0(a, c - b, c) = \Omega_0(c - a, c - b, c)$, for integers a, b, c with $0 < a \leq b \leq c$.

The rest of this section reviews some results from (Brimkov and Barneva 2004). The following theorem provides reachable upper and lower bounds for the connectivity number.

Theorem 34 $a - 1 \leq \Omega_0(a, b, c) \leq b - 1$, if $a + b < c < a + 2b$.

(Brimkov and Barneva 2004) also provides an algorithm computing $\Omega_0(a, b, c)$ with $O(a \log b)$ arithmetic operations, where $0 \leq a \leq b \leq c$. Within a model with a unit cost floor operation, the algorithm complexity is $O(a)$.

The following theorem provides an explicit solution under certain conditions.

Theorem 35 (Brimkov and Barneva 2004) Let a, b, c be relatively prime in-

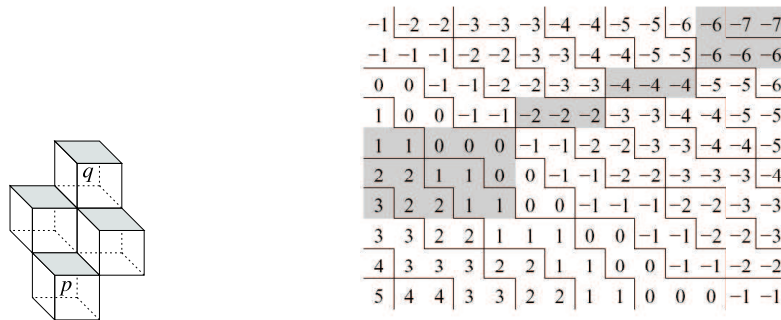


Fig. 10. *Left*: A jump; *Right*: Height map of the naive plane $D_{5,7,11,0,11}$: the 0-connected set of pixels (shown in gray) is a projection of a 0-disconnected set of voxels of this naive plane (Brimkov and Barneva 2004).

tegers with $c \geq a + 2b$ and $0 < a \leq b \leq c$. Then $\Omega_0(a, b, c) = c - a - b + \gcd(a, b) - 1$.

PROOF. Let A be a 2D array (finite or infinite) and $p = (x_0, y_0)$, $q = (x_m, y_m)$ two points of A . Let, for definiteness, $x_0 \leq x_m$ and $y_0 \leq y_m$. The sequence of points $P = \langle (x_0, y_0) = p, (x_1, y_1), (x_2, y_2), \dots, (x_m, y_m) = q \rangle$ is a *stairwise path* between p and q if the coordinates of two consecutive points (x_i, y_i) and (x_{i+1}, y_{i+1}) , $0 \leq i \leq m - 1$, satisfy either $x_{i+1} = x_i, y_{i+1} = y_i + 1$, or $x_{i+1} = x_i + 1, y_{i+1} = y_i$. The number m is the *length* of the path. For all other possible mutual locations of p and q , a stairwise path is defined similarly (see Figure 11 (Left)).

Consider now the remainder map $M_{a,b,c}^{(rem)}$ together with its equivalence classes described above. The points of $M_{a,b,c}^{(rem)}$ which contain the value $\Omega_0(a, b, c)$ are called the *plugs* of $M_{a,b,c}^{(rem)}$. The points containing the maximal possible value $c - 1$ are the *maximal points* of $M_{a,b,c}^{(rem)}$. Assume for a moment that c is “enough large” compared to a and b . More precisely, suppose that $c \geq a + 2b$. Then the digital lines corresponding to the equivalence classes are thicker than standard. In particular, if $c = a + 2b = (a + b) + b$, then a particular equivalence class C is a disjoint union of one standard and one naive line. Note that in this case there are two different possible partitions of this kind: one can consider the standard line to be above the naive, and vice versa. In the first case we call the standard line *upper standard line* for the class C . We will use it in the rest of the proof. Similarly, if $c > a + 2b$, then C can be partitioned in two different fashions into disjoint union of one standard line and another line which is thicker than naive. Consider then a class C which contains maximal points of $M_{a,b,c}^{(rem)}$, where $c \geq a + 2b$. We have $C = S \cup L$, $S \cap L = \emptyset$, where S is

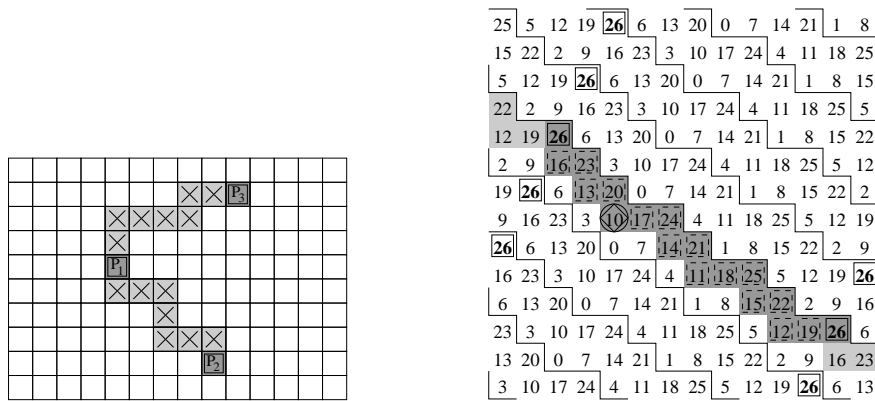


Fig. 11. *Left:* Two stairwise paths marked by shadowed \times sign: one between the points P_1 and P_2 , and another between the points P_1 and P_3 ; *Right:* A stairwise path between two maximal points of value 26 in array $M_{7,10,27}^{(rem)}$. The path (in dark gray) is a part of an upper standard line (in gray) through the two maximal points. The core of the class has value 10. It coincides with a plug of $M_{7,10,27}^{(rem)}$. A core is marked by \diamond and a plug by \times .

the standard line containing maximal points of $M_{a,b,c}^{(rem)}$, and L is a digital line that is naive or thicker than naive. It is composed by the pixels that belong to the complement of S to C and are “below” S (see Figure 11 (*Right*)). A point $P \in S$ with a minimal value is called a *core of the class C* (Figure 11 (*Right*)). Keeping in mind the properties of $M_{a,b,c}^{(rem)}$, we can state the following lemma.

Lemma 36 *Let P_1 and P_2 be two consecutive (by position) maximal points belonging to an equivalence class C . Let $S \subseteq C$ be the standard line containing P_1 and P_2 , and $\bar{S}(P_1, P_2) \subset S$ the stairwise path between P_1 and P_2 . Then:*

- (1) *All points of S have different values;*
- (2) *\bar{S} contains $\frac{a+b}{\gcd(a,b)}$ points with values $c-1, c-1-\gcd(a,b), c-1-2\gcd(a,b), \dots, f$, where the last value f is equal to*

$$f = c - 1 - \left(\frac{a+b}{\gcd(a,b)} - 1 \right) \gcd(a,b) = c - a - b + \gcd(a,b) - 1$$

See Figure 11 (*Right*). To complete the proof of the theorem, let the points $P_1, P_2 \in C$, the standard line S , and the stairwise path $\bar{S}(P_1, P_2)$ be as in Lemma 36. This last lemma implies that \bar{S} contains a unique core of C . Clearly, when ω decreases starting from $c-1$ and going downwards, first the points from the standard line S will vanish from $M_{a,b,c}^{(rem)}$. Consider first what happens when $c = a + 2b$. As already discussed above, the complement of S to C is a naive line L which is “below” S . Moreover, the mutual location of S and L within the class C implies the following property: The 1-neighbors of any pixel from S are points which belong either to S or to L . See Figure 11 (*Right*). Therefore, if the points of S are removed from C , all points of the naive line L will be disconnected from the points of the next equivalence class “above” C . Obviously, this will also hold when $c > a + 2b$. All equivalence classes are digital lines and therefore are periodic. The period length of a class is equal to $a + b$ which is the length of the path between two consecutive maximal points of C . Therefore, the disconnectedness considered above propagates along all the class C . On the other hand, the array of remainders $M_{a,b,c}^{(rem)}$ is periodic, as the class C appears periodically in a way that if we start counting from it, every $\gcd(a,b)$ th class is equivalent to C . Thus we obtain that if $c \geq a + 2b$, the array $M_{a,b,c}^{(rem)}$ becomes disconnected when the points of the standard line S are removed from it.

What remains to show is that $\Omega_0(a, b, c) = c - a - b + \gcd(a, b) - 1$. Clearly, the value of $\Omega_0(a, b, c)$ is equal to the value of a core of a class C that contains maximal values. In other words, we have that the set of plugs of $M_{a,b,c}^{(rem)}$ coincides with the set of the cores of all classes containing maximal elements. If $\gcd(a, b) = 1$, then $\Omega_0(a, b, c) = c - a - b = c - a - b + \gcd(a, b) - 1$, since $M_{a,b,c}^{(rem)}$ becomes disconnected when points with values $c-1, c-2, \dots, c-a-b$

are removed from it. Now let $\gcd(a, b) = d \neq 1$. Consider again the points in a stairwise path $\bar{S}(P_1, P_2)$ between two consecutive maximal points in a class C . Then part 2 of Lemma 36 implies that if $c \geq a + 2b$, then $\Omega_0(a, b, c) = c - a - b + \gcd(a, b) - 1$. \square

This theorem combined with Proposition 33 allows to derive further explicit solutions, such as

$$\begin{aligned}\Omega_0(a, b, c) &= b - a + \gcd(a, c - b) - 1, \text{ if } c < 2b - a \\ \Omega_0(a, b, c) &= b + a - c + \gcd(c - b, c - a) - 1, \text{ if } c < a + b/2\end{aligned}$$

and the lower bound

$$\Omega_0(a, b, c) \geq c - a - b + \gcd(a, b) - 1 \text{ for any } a, b, c$$

7 Algorithms

Theoretical research on digital planarity is naturally driven by important practical applications in image analysis, pattern recognition and volume modeling. In this section we review some basic algorithms for digital plane recognition, digital surface segmentation, and digital polyhedra generation.

7.1 DPS Preimage Analysis

Let S be a digital plane segment defined by an Euclidean plane $\Gamma(\alpha_1, \alpha_2, \beta)$ with $0 \leq \alpha_1 \leq 1$, $0 \leq \alpha_2 \leq 1$ and $0 \leq \beta < 1$.

Definition 37 (Vittone and Chassery 2000) The preimage of a DPS S is the set of points $(\alpha_1, \alpha_2, \beta) \in [0, 1]^2 \times [0, 1[$, such that $S \subset I_{\alpha_1, \alpha_2, \beta}$.

In other words, the preimage is the set of Euclidean planes whose digitizations contain S . According to this definition and the discussion related to Theorem 10, the preimage is the solution of a system of linear inequalities with unknowns α_1, α_2 , and β . Thus it is a convex polyhedron (possibly empty). To compute the preimage, we use the linear *dual transform* that maps an Euclidean plane $\Gamma(\alpha_1, \alpha_2, \beta)$ in \mathbb{R}^3 to the point $(\alpha_1, \alpha_2, \beta)$ in the parameter space, also called *dual space*. Conversely, the dual transform of plane in the dual space is a point in \mathbb{R}^3 (also called *primal space*). The dual transform is a classical tool in computational geometry to solve linear programming problems (Preparata and Shamos 1985).

In dimension 2, the analysis of the preimage structure allowed to design efficient recognition algorithms. Indeed, the preimage associated to a given 0-arc has a robust arithmetic structure (describable by means of Farey cells). Moreover, the number of vertices of this domain is bounded by 4 (Dorst and Smeulders 1984) (McIlroy 1985) (Lindenbaum and Bruckstein 1993). Beside the arithmetic properties of the preimage, the bound on the number of vertices induces a linear-time (i.e., the processing time for each new vertex is a constant) on-line algorithm to compute and update the 2D preimage, and thus to decide whether a 0-arc is a digital straight segment or not.

Arithmetic properties of preimages and their geometry in 3D are not yet studied extensively. Consider the digital plane segment $S \subset D_{a,b,c,\mu,c}$ (again, without loss of generality, we suppose that $0 \leq a \leq b < c$). From the remainder map associated to S (see Section 4), we can define the *lower* (resp. *upper*) *supporting points* whose remainder $r = ax + by + cz$ is μ (resp. $\mu + c - 1$). For the sake of clarity, we suppose that S contains at least three upper and three lower supporting points. The analysis from (Coeurjolly et al. 2005) is based on the following proposition.

Proposition 38 (Coeurjolly et al. 2005) *Let $S \subset D_{a,b,c,\mu,c}$ be a DPS. Then, the preimage of S , denoted $\mathcal{P}(S)$, containing all the Euclidean planes in the parameter space, has the following properties:*

- *Points $v_l = (\frac{a}{c}, \frac{b}{c}, \frac{\mu}{c})$ and $v_u = (\frac{a}{c}, \frac{b}{c}, \frac{\mu+1}{c})$ are vertices of $\mathcal{P}(S)$; v_l (resp. v_u) is the dual transform of the lower (resp. upper) supporting planes $ax+by+cz = \mu$ (resp. $ax + by + cz = \mu + c$) in the primal space (i.e., the one to which $D_{a,b,c,\mu,c}$ belongs);*
- *The planes in the dual space supporting faces of the preimage adjacent to v_l (resp. v_u) are the dual transforms of the vertices of the 2D convex hull of the lower (resp. upper) supporting points in S .*

An illustration to the 2D convex hulls is given in Figure 12. As a consequence of this proposition, the number of preimage faces is at least the number of vertices of the convex hull of the upper 2D supporting points plus the number of vertices of the convex hull of the lower 2D supporting points. (Coeurjolly et al. 2005) also proves that for a given class of digital plane segments, the preimage does not have other faces than those induced by supporting points. However, a general result with a specific recognition algorithm is still a challenging task.

7.2 DPS Recognition and Digital Surface Segmentation

DPS recognition and digital surface segmentation are fundamental problems in image analysis. Table 1 lists different algorithms and their computational

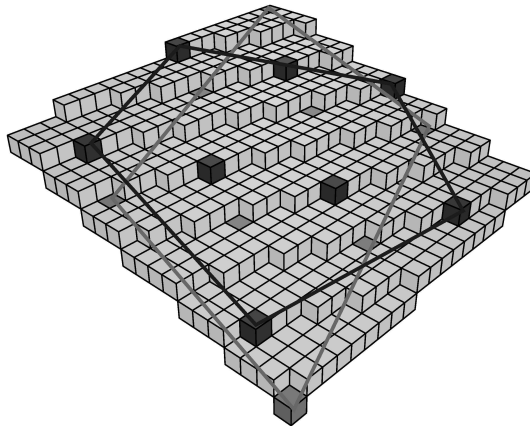


Fig. 12. Illustration of a subset of a digital plane $D_{7,17,57,0,57}$ with its lower and upper convex hulls on the supporting planes.

costs. All complexity bounds are given with respect to the number n of grid points in S . The fourth column indicates whether the algorithm performs (just) a coplanarity test (\mathcal{T}) with respect to a digital plane (note that coplanar voxels are not necessarily connected), or may even lead to a complete recognition (\mathcal{R}) (connectivity of the voxels is required). Note that any \mathcal{T} algorithm (that also takes connectivity into account) is an \mathcal{R} algorithm as well.

Theorem 12 has been used in (Stojmenović and Tosić 1991) to support a DPS recognition algorithm based on convex hull separability. The recognition of DPSs in grid adjacency models is discussed in (Veelaert 1994) (applying the characterization by evenness as discussed in Section 2), (Klette et al. 1996) (recognition by least-square optimization), and (Megiddo 1984), (Preparata and Shamos 1985), (Vittone and Chassery 2000), (Buzer 2002) (linear programming when the dimension is fixed). (Debled-Renesson and Reveillès 1994) proposes an approach based on tests for existence of lower and upper supporting planes for the given set of points.

(Françon et al. 1996) suggests a recognition method for DPSs by converting the problem into a system of n^2 linear inequalities, where n is the cardinality of the given set of points. The system is solved by the Fourier elimination algorithm. One can also apply the CDD algorithm⁸ for solving systems of linear inequalities by successive intersection of half-spaces defined by inequalities (Fukuda and Prodon 1996). A very efficient incremental algorithm based on a similar approach is proposed in (Klette and Sun 2001). Typical timing results for these three versions are shown in Figure 13, using a polyhedrized digital ellipsoid at grid resolutions ranging from 10 to 100. In what follows we present more in detail the algorithm from (Klette and Sun 2001), which appears to be superior to the others.

⁸ **C** implementation of the **D**ouble **D**escription (CDD) Method of Motzkin et al., see http://www.ifor.math.ethz.ch/~fukuda/cdd_home/cdd.html

Main reference	Description	Complexity	\mathcal{T} or \mathcal{R}	Comments
(Kim 1984)	Detection of a supporting plane	$O(n^4)$	\mathcal{T}	Based on an incorrect theorem
(Megiddo 1984)	Linear programming	$O(n)$	\mathcal{T}	
(Preparata and Shamos 1985)	Linear programming	$O(n \log n)$	\mathcal{T}	Provides the complete preimage
(Kim 1991)	Detection of a supporting plane	$O(n^2 \log n)$	\mathcal{T}	Optimization of (Kim 1984), also based on an incorrect theorem
(Stojmenović and Tosić 1991)	Convex hull separability	$O(n \log n)$	\mathcal{T}	
(Veelaert 1994)	Evenness property	$O(n^2)$	\mathcal{R}	Rectangular DPS
(Debled-Renesson and Reveillès 1994)	Arithmetic structure	n.a.	\mathcal{R}	Rectangular DPS
(Reveillès 1995)	Arithmetic geometry	$O(n)$	\mathcal{R}	Rectangular DPS
(Vittone and Chassery 2000)	Linear programming and Farey series	$O(n^3 \log n)$	\mathcal{T}	Preimage computation with arithmetic solutions
(Klette and Sun 2001)	Combinatorial procedure	n.a.	\mathcal{R}	
(Buzer 2002)	Linear programming for DPS recognition	$O(n)$	\mathcal{T}	On-line algorithm
(Gérard et al. 2005)	Convex hull analysis	$O(n^7)$	\mathcal{T}	fast algorithm in practice

Table 1
Algorithms for DPS recognition.

Algorithm KS2001

Following Section 3, an Euclidean plane Π is a supporting plane of a finite set of faces, if all the faces are in one of the closed halfspaces defined by Π , and the main diagonal distance of any vertex of these faces to Π is less than $\sqrt{3}$. It can be shown that if the set of faces has $n \geq 4$ vertices, then a supporting plane exists iff there is a supporting plane Π which is incident with three non-collinear vertices of the given set of faces. A set of faces can have more than

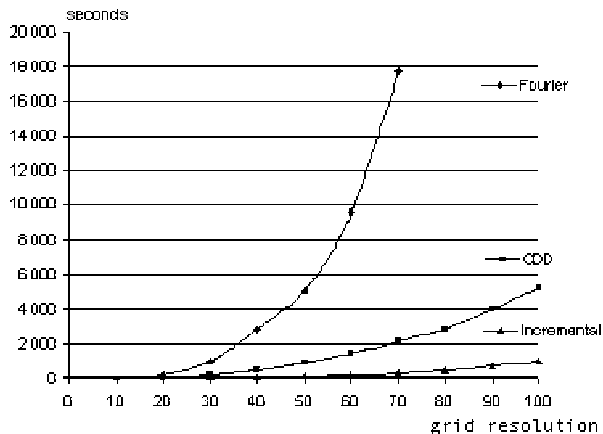


Fig. 13. Running times of three DPS recognition algorithms on a PIII 450 running Linux (Klette and Sun 2001). (*L. Papier* provided the Fourier elimination program.)

one supporting plane of this kind.

A DPS in the incidence grid is (without loss of generality) a 1-connected set of 2-cells in the frontier of a 2-region of voxels. A *simply-connected DPS* consists of faces whose union is homeomorphic to the unit disk, i.e., it is a 1-simply-connected set of 2-cells.

If we are given the frontier of the projection of the DPS onto a supporting plane, it is possible to reconstruct the DPS in the 3D space (up to a translation in the normal direction to the planes). A supporting plane and a parallel plane in main diagonal distance less than, or equal to $\sqrt{3}$ define a *pair of parallel planes*.

Let \mathbf{v} be the vector of length $\sqrt{3}$ in the main diagonal direction and let \mathbf{n} be an outward pointing normal to the pair of parallel planes. Furthermore, for a vertex \mathbf{p} incident with the DPS of 2-cells, let $\mathbf{v} \cdot \mathbf{p} = d_{\mathbf{p}}$ be the equation of a plane with normal \mathbf{v} and incident with \mathbf{p} . The vertices \mathbf{p} of the grid faces of a DPS must satisfy

$$0 \leq \mathbf{n} \cdot \mathbf{p} - d_{\mathbf{p}} < \mathbf{n} \cdot \mathbf{v} \quad (6)$$

Let $\mathbf{n} = (a, b, c)$. The scalars a, b, c may have different signs, but since \mathbf{n} and \mathbf{v} must point into the same direction “modulo a directed diagonal,” without loss of generality we can assume that $a, b, c > 0$. Condition (6) then becomes

$$0 \leq ax + by + cz - d_{\mathbf{p}} < a + b + c \quad (7)$$

Hence, a DPS in the grid-cell model is equivalent (by mapping vertices into grid points) to a finite 2-connected set of grid cells in a standard digital plane (see Definition 13), with $\nu = d_{\mathbf{p}}$ and $\omega = a + b + c$.

In addition to checking the tripod condition (which is easy), the task of DPS

recognition (in the grid-cell model) can be solved by answering the following question: Given n vertices $\{p_1, p_2, \dots, p_n\}$, does each p_i with $d_i = \mathbf{v} \cdot p_i$ satisfy Condition (6), i.e., do we have

$$0 \leq \mathbf{n} \cdot p_i - d_i < \mathbf{n} \cdot \mathbf{v} \quad \text{for } i = 1, \dots, n? \quad (8)$$

The incremental algorithm repeatedly updates a list of supporting planes; if the list is empty, the set of points is not a DPS. The updating step is as follows: If we have $n \geq 0$ points, we add an $(n + 1)$ st point iff the list of supporting planes remains non-empty. To test this, we first check the new point against each of the listed supporting planes to see if it is on the same side of the plane as the other points and within the allowed diagonal distance. If these conditions are not satisfied, we delete the plane from the list. We then construct new supporting planes by combining the new point with selected pairs (see below) of existing points. A new supporting plane is added to the list if all $n + 1$ points satisfy the conditions. The set of points is accepted as a DPS iff the final list of planes is non-empty. The updating step is time-efficient because we can restrict the tests to points that have extreme positions in any of the eight diagonal directions.

A given frontier S of a 2-component of voxels consists of 1-connected 2-cells. These faces can be represented by a face graph whose nodes are the faces and where each node has uniformly four pointers to its four 1-adjacent faces. The face graph can be constructed using (e.g.) the Artzy-Herman surface tracing algorithm (Artzy et al. 1981), which only requires two visits of each face.

We can perform a breadth-first search of the face graph to agglomerate the faces into DPSs. The second process is implemented using two queues. The first is called a *seeds queue*; it contains all the faces found by the search which do not belong to any yet recognized DPS.

A face is inserted into the seeds queue if it cannot be added to the current

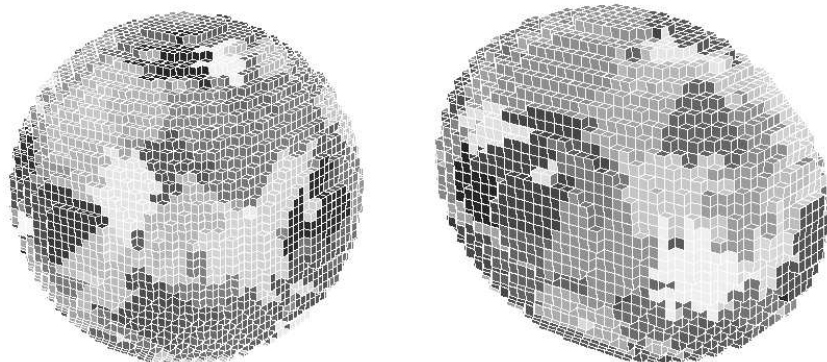


Fig. 14. Agglomeration into DPSs of the faces of a sphere and an ellipsoid (grid resolution $h = 40$) (Klette and Sun 2001).

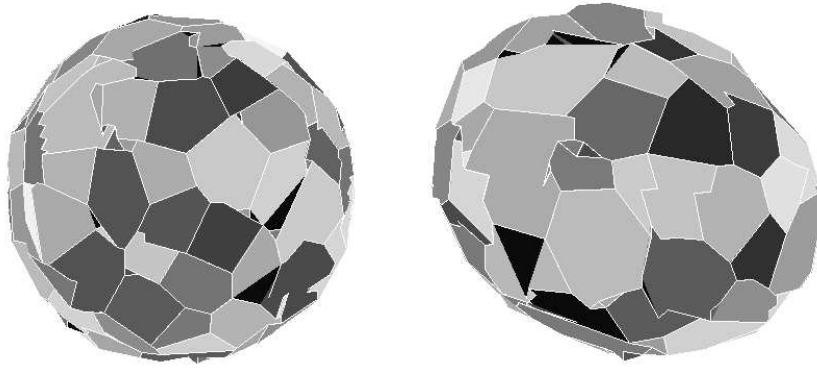


Fig. 15. A polyhedrized sphere and ellipsoid (Klette and Sun 2001).

DPS. The next DPS starts from a face chosen from the seeds queue; the choice of this face determines how the DPS “grows.” The second queue is used to maintain the breadth-first search. “Growing a DPS” looks like propagating a “circular wave” on S from a center at the original seed face.

We try to add an adjacent face to the current DPS by testing each vertex of the face that is not yet on the DPS. If all four vertices pass the test, the face is added to the DPS and deleted from the seeds queue (if it was on that queue). Otherwise, we insert the face into the seeds queue and test another adjacent face. If no more adjacent faces can be added, we start a new DPS from a face on the seeds queue.

A list of the frontier vertices of each DPS is maintained during the agglomeration process, not only to simplify the tests of whether a new vertex can be added, but also to maintain the homeomorphism of the DPS to a unit disk. This ensures that the frontier always remains a simple polygon, so that the algorithm constructs only simply-connected DPSs. (This condition can be removed, if desired.)

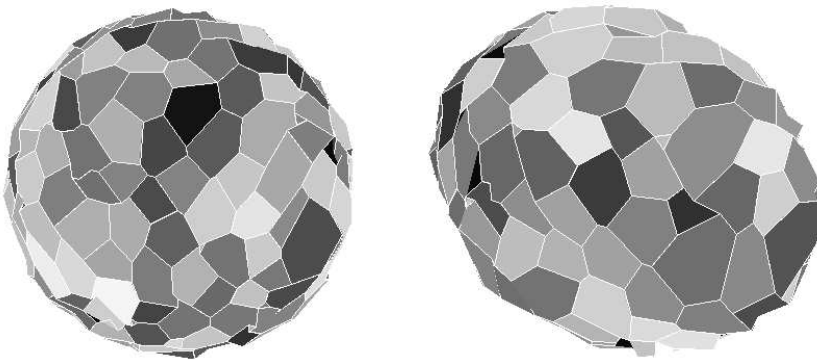


Fig. 16. The polyhedrized sphere and ellipsoid where the breadth-first search depth is restricted to 7 (Klette and Sun 2001).

Figure 14 illustrates results of the agglomeration process for a digitized sphere and for an ellipsoid with semi-axes 20, 16, and 12. Faces that have the same gray level belong to the same DPS. The respective numbers of faces of the digital surfaces of the sphere and ellipsoid are 7,584 and 4,744, respectively. The numbers of DPSs are 285 and 197; the average sizes of these DPSs are 27 and 24 faces.

To complete the polyhedrization process, we set all the face vertices that are incident with at least three of the DPSs to be vertices of the polyhedron. Figure 15 shows the final polyhedral surfaces generated for the sphere and ellipsoid. Note that these polyhedral surfaces are not simple (they are not homeomorphic to the surface of a unit sphere; they have holes; see, e.g., (Klette and Rosenfeld 2004) for more on simple surfaces and holes).

Restricting the depth of the breadth-first search changes the polyhedrization from global to local and results in “more uniform” polyhedra. Figure 16 shows results when the depth is restricted to 7. The number of small DPSs is reduced and the sizes of the DPSs are more evenly distributed. The respective numbers of DPSs are 282 and 180 and their average sizes are 27 and 26; note that these are nearly the same as in the unrestricted case.

As mentioned above, the output of Algorithm KS2001 is in general not a valid polyhedron but like a *patchwork* of planar segments. It is desirable to obtain a polyhedron with the following reversibility property: the polyhedron digitization coincides with the originally given set of grid points. Below we sketch an algorithm from (Coeurjolly et al. 2004) that addresses the problem of such a reversible polyhedrization.

Algorithm CGS2004

The main idea is to simplify the polyhedron obtained by a Marching-Cubes (MC) algorithm (Lorensen and Cline 1987), using information about the digital surface segmentation. The MC algorithm is a widely used isosurface generation algorithm in 3D volume data. This method considers local grid point configurations to replace them by small triangles composing the global isosurface. With a reference to (Lachaud and Montanvert 2000), the triangulated surface obtained by the MC algorithm is a combinatorial 2-manifold. In other words, the surface is closed, hole-free and without self-crossing. Furthermore, the object boundary quantization (OBQ) of this polyhedron is exactly the input binary object.

Let us consider a voxel p from the object boundary and a voxel q from the background, such that the L_1 distance between p and q is 1. Both voxels define a segment $]pq[$ (see Figure 18-*left*). Note that every MC vertex belongs to a distinct $]pq[$ segment. More precisely, a MC vertex can be attached

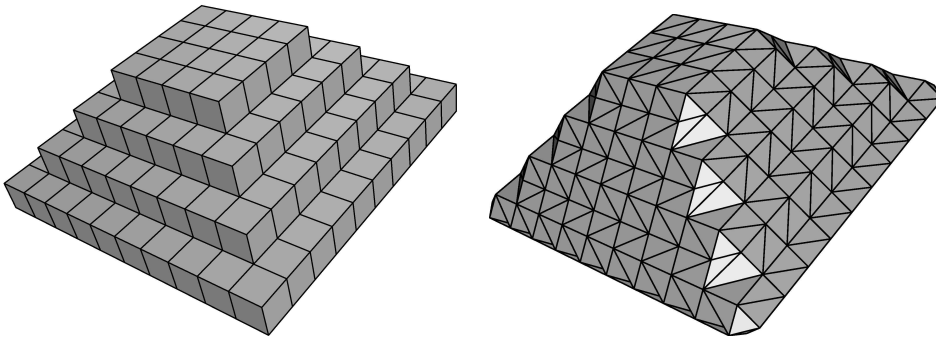


Fig. 17. A $\{0,1\}$ -binary object and a Marching-Cubes surface obtained with an iso-level in $]0, 1[$.

to each boundary surface element. In (Lachaud and Montanvert 2000) it is proved that the MC surface is a combinatorial 2-manifold, independently of the position of the vertices in the $]pq[$ segments. Furthermore, a vertex displacement along the $]pq[$ does not change the reversibility property.

To link all these properties to the polyhedrization problem, we consider a set S of voxels from the object boundary such that S is a DPS, and π is a Euclidean plane from the DPS preimage (we also suppose that π does not belong to the preimage boundary). It can be proved that π intersects each segment $]pq[$ for each p in S . Let \mathcal{P} be the polyhedron given by projecting the MC vertices associated to S onto π along the $]pq[$ segments. Then it can be proved that \mathcal{P} is a combinatorial 2-manifold that still has the reversibility property. Moreover, all the triangles associated to the set S are coplanar. The last step of the algorithm consists of merging the coplanar triangles associated to S while preserving the topology of the surface. The projection operation and the merging steps are repeated for every recognized digital plane.

The output of the algorithm is a digital polyhedron such that a large facet is associated to each recognized DPS. The facets of the polyhedron are stitched together by strips of triangles. These triangles are called *non-homogeneous* in (Coeurjolly et al. 2004) because their three vertices do not belong to the same digital plane. The obtained polyhedron is a combinatorial 2-manifold and possesses the reversibility property.

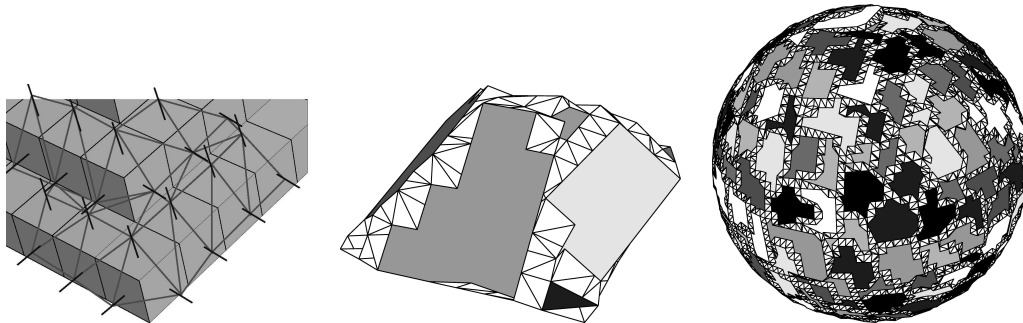


Fig. 18. *From left to right*: links between MC vertices and $]pq[$ segments, final result on the object of Figure 17, and result on a sphere of radius 25.

In this section we briefly consider certain problems that are in a sense reverse to those of the previous section. One of these is DPS generation. Usually straightforward methods for its solution directly follow from the particular definition of a digital plane. See, e.g., (Debled-Renesson and Reveillès 1994) for an algorithm based on Reveillès definition of arithmetic planes. A related problem is the digitization (scan-conversion) of a given space polygon. An efficient practical algorithm has been proposed in (Kaufman 1987). Algorithms involving “supercovers” (i.e., “thick” digitizations including all voxels intersected by the given polygon) have been proposed in (Andres et al. 1997a). Discrete linear manifolds within a “standard model” (i.e., based on standard planes) have been defined in (Andres 2003).

For various applications in surface modeling it is reasonable to work with an appropriate polyhedral approximation of a given surface rather than with the surface itself. Often this is the only possibility since the surface may not be available in an explicit form. Thus having suitable algorithms for digitizing a polyhedral surface is of significant practical importance. The above-mentioned supercover approach has been applied to polyhedra digitization (Andres et al. 1997b). The faces of the obtained digital polyhedra admit analytical description. They are portions of planes’ supercovers that are thicker than the (naive) digital planes. As discussed in the literature, the optimal ground for polyhedra digitization is naturally provided by the naive digital planes. However, it has been unclear for a long time how to define a “naive” digital polygon and especially its edges, so that the overall digitization to admit no gaps along the edges of the resulting digital polyhedron. These theoretical obstacles have been recently overcome by employing relevant mathematical approaches. Specifically, three different algorithms have been proposed. The first one (Barneva et al. 2000) is based on reducing the 3D problem to a 2D one by projecting the surface polygons on suitable coordinate planes, next digitizing the obtained 2D polygons, and then restoring the 3D digital polygons. The generated digital polygons are portions of the naive planes associated with the facets of the surface. Another algorithm (Brimkov and Barneva 2002) is based on introducing new classes of 3D lines and planes (called *graceful*) which are used to approximate the surface polygons and their edges, respectively. The algorithm from (Brimkov et al. 2000b) approximates directly every space polygon by a digital one, which is again the thinnest possible, while the polygons’ edges are approximated by the thinnest possible naive 3D straight lines defined algorithmically in (Kaufman and Shimony 1986) and analytically in (Figueiredo and Reveillès 1995) and (Brimkov et al. 2000b). All these algorithms assure 2-gapfree discretizations. They run in time that is linear in the number of the generated voxels, which are stored in a 2D array. Moreover, the generated 3D digital polygons admit analytical description.

In the remainder of this section we briefly describe the algorithm from

(Brimkov et al. 2000b). Our choice is dictated by the fact that this algorithm provides an “optimal solution” while being optimally fast and using memory space of optimal order. In fact, the obtained discretization appears to be *minimally thin*, in a sense that removing an arbitrary voxel from the digital surface leads to occurrence of a 2-gap in it.

Algorithm BBN2000

For the sake of simplicity, consider a polyhedral surface which is a mesh of triangles. As mentioned, the triangles’ sides are modeled by naive 3D lines and their interiors by naive planes. Naive 3D lines have been first defined algorithmically in (Kaufman and Shimony 1986). Given a Euclidean straight line L determined by a vector (a, b, c) with $0 \leq a \leq b \leq c$, the digitization of L by truncation is the set of voxels (x, y, z) with coordinates $x = \lfloor \frac{ai}{c} \rfloor, y = \lfloor \frac{bi}{c} \rfloor, z = i, i \in \mathbb{Z}$. This digital line is 0-connected and “minimal” in a sense that the removal of any element splits the set into two separate 0-connected components. It can analytically be defined by $0 \leq -cx + az + \lfloor \frac{c}{2} \rfloor < c, 0 \leq -cy + bz + \lfloor \frac{c}{2} \rfloor < c$. Such a digital 3D line is called *regular* and denoted by L_R . It is centered about the continuous line L and every voxel of L_R is intersected by L . A regular naive line through two points A and B is denoted $L_R(AB)$ (see Figure 19 on the left).

The construction of the triangle interior is somewhat more sophisticated. Recall that an arithmetic plane $P = P_{a,b,c,\mu,\omega}$ is *functional* over a coordinate plane, say, xy , if for any pixel (x, y) from xy there is exactly one voxel belonging to P . The coordinate plane xy is called *functional plane* for P and denoted by π_P . Consider first a 2D Euclidean triangle $\Delta A'B'C'$ in the xy -plane. We define the *integer set* $I_{2D}\Delta A'B'C'$ of $\Delta A'B'C'$ as the set of all integer points which belong to the interior *or* the sides of $\Delta A'B'C'$. Thus, in particular, the vertices A', B' , and C' belong to $I_{2D}\Delta A'B'C'$ (see Figure 19, middle). The 3D triangle is a portion of a special kind of naive plane $P_{a,b,c,\mu+\lfloor \frac{c}{2} \rfloor, c}$, centered about the Euclidean plane and called *regular*. A regular plane through the points A, B, C is denoted P_R^{ABC} . Then an *integer set* of a 3D triangle ΔABC is defined as follows. Let A', B' , and C' be the projections of A, B and C onto $\pi_{P_R^{ABC}}$ and $I_{2D}\Delta A'B'C'$ the integer set of $\Delta A'B'C'$. Then the *integer set* $I_{3D}\Delta ABC$ of ΔABC is the set of voxels belonging to P_R^{ABC} and whose projections on $\pi_{P_R^{ABC}}$ constitute exactly the set $I_{2D}\Delta A'B'C'$. Note that the centers of the voxels of the integer set of ΔABC do not necessarily belong to ΔABC . With this preparation, a *3D digital triangle* $T(ABC)$ is defined as the union of its sides $L_R(AB), L_R(AC)$, and $L_R(BC)$ and the integer set $I_{3D}\Delta ABC$. Note that the discrete sides of $T(ABC)$ and the integer set of ΔABC may contain common voxels (see Figure 19, middle).

The above constructive definition infers an algorithm for digitization of triangles and meshes of triangles. Let a mesh of a finite number of 3D triangles be

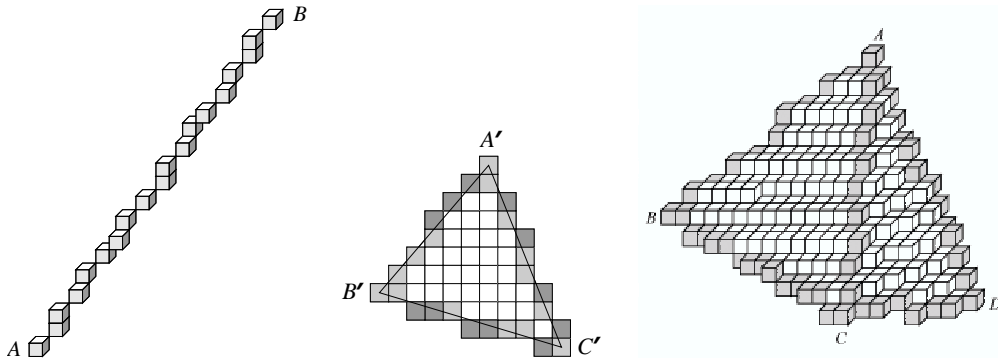


Fig. 19. *Left*: A regular naive 3D line between the points $A = (0, 0, 0)$ and $B = (11, 13, 18)$; *Middle*: Projection of digital triangle $T(ABC)$ on the functional plane. The white pixels belong to $I_{2D}\Delta A'B'C'$ but do not correspond to sides of $T(ABC)$. Dark gray pixels correspond to sides of $T(ABC)$ but do not belong to $I_{2D}\Delta(A'B'C')$. Light gray pixels are in $I_{2D}\Delta A'B'C'$ and correspond to sides of $T(ABC)$; *Right*: Mesh of two 3D digital triangles $T(ABC)$ and $T(ABD)$, obtained by the described algorithm. The mesh vertices are $A = (1, 8, 6)$, $B = (-8, -2, 0)$, $C(7, -8, -4)$, and $D(14, -4, -5)$.

given. Each triangle is specified by its three vertices that are supposed to be integer points. A triangle ΔABC in the 3D space is then digitized as follows.

- (i) Approximate the sides AB , AC , and BC by the corresponding regular 3D lines $L_R(AB)$, $L_R(AC)$, and $L_R(BC)$;
- (ii) Determine the regular plane P_R^{ABC} ;
- (iii) Find the functional plane $\pi_{P_R^{ABC}}$ of P_R^{ABC} ;
- (iv) Find the respective projections A' , B' , and C' of A , B , and C on $\pi_{P_R^{ABC}}$;
- (v) Determine the integer set $I_{2D}\Delta A'B'C'$ of $\Delta A'B'C'$;
- (vi) Generate the integer set $I_{3D}\Delta ABC$ of ΔABC from $I_{2D}\Delta A'B'C'$.

The union of the sides and the integer set constitutes the digital triangle $T(ABC)$. Then the triangular mesh voxelization is obtained by digitizing every triangle of the mesh. It is proved that a digital triangle generated by the above algorithm is 2-gapfree and that the obtained triangular mesh voxelization is 2-gapfree, as well. Moreover, removal of an arbitrary voxel from the obtained digital polyhedral surface causes occurrence of a 2-gap. The algorithm has linear time and space complexity in the number of the generated voxels. An example of a mesh of two digital triangles obtained through the proposed algorithm, is outlined in Figure 19 on the right.

8 Conclusions

Digital planarity is expected to be an even more challenging subject than digital straightness. It seems to be far from fully explored, and the authors expect further valuable contributions to this subject in near future. This article

may help to focus research on important open issues such as number-theoretic characterizations or a wider collection of recognition algorithms with a more detailed comparative evaluation. Segmentations of 3D surfaces into DPSs will become increasingly important. Characterizations of such segmentations (e.g., “balanced in size,” or “approximating convex faces”), as well as algorithms that optimize such kind of properties, are of significant interest.

Acknowledgments

End of 2003 the late Azriel Rosenfeld agreed to use parts of chapters 11 and 12 of (Klette and Rosenfeld 2004) for this reviewing article. The authors dedicate it to this outstanding researcher who established the field of digital geometry with numerous fundamental contributions. The authors also thank the reviewers for careful reading and their comments.

References

1940-1959

[Morse and Hedlund 1940] M. Morse and G. A. Hedlund. Symbolic dynamics II: Sturmian sequences. *Amer. J. Math.*, **61**:1–42, 1940.

1960-1969

[Freeman 1961] H. Freeman. Techniques for the digital computer analysis of chain-encoded arbitrary plane curves. *Proc. Natl. Elect. Conf.*, **17**:421–432, 1961.

[Blankinship 1963] W. A. Blankinship. A new version of the Euclidean algorithm. *Amer. Math. Monthly*, **70**:742–745, 1963.

1970-1979

[Brons 1974] R. Brons. Linguistic methods for description of a straight line on a grid. *Computer Graphics Image Processing*, **2**:48–62, 1974.

1980-1989

[Artzy et al. 1981] E. Artzy, G. Frieder, and G. T. Herman. The theory, design, implementation and evaluation of a three-dimensional surface detection algorithm. *Computer Vision, Graphics, Image Processing*, **15**:1–24, 1981.

[Kim and Rosenfeld 1982] C. E. Kim and R. Rosenfeld. Convex digital solids. *IEEE Trans. Pattern Analysis Machine Intelligence*, **4**:612–618, 1982.

[Megiddo 1983] N. Megiddo. Linear-time algorithms for linear programming in \mathbb{R}^3 and related problems. *SIAM J. Computing*, **12**:759–776, 1983.

[Dorst and Smeulders 1984] L. Dorst and A. W. M Smeulders. Discrete representation of straight lines. *IEEE Trans. Pattern Analysis Machine Intelligence*, **6**:450–463, 1984.

- [Kim 1984] C. E. Kim. Three-dimensional digital planes. *IEEE Trans. Pattern Analysis Machine Intelligence*, **6**:639–645, 1984.
- [Megiddo 1984] N. Megiddo. Linear programming in linear time when the dimension is fixed. *J. ACM*, **31**:114–127, 1984.
- [Hung 1985] S. H. Y. Hung. On the straightness of digital arcs. *IEEE Trans. Pattern Analysis Machine Intelligence*, **7**:203–215, 1985.
- [McIlroy 1985] M. D. McIlroy. A note on discrete representation of lines. *AT&T Technical J.*, **64**:481–490, 1985.
- [Preparata and Shamos 1985] F. P. Preparata and M. I. Shamos. *Computational Geometry: An Introduction*. Springer, New York, 1985.
- [Kaufman and Shimony 1986] A. Kaufman and E. Shimony. 3D scan-conversion algorithms for voxel-based graphics. In Proc. *Workshop on Interactive 3D Graphics*, pages 45–75, ACM, New York, 1986.
- [Kaufman 1987] A. Kaufman. An algorithm for 3D scan-conversion of polygons. In Proc. *Eurographics*, pages 197–208, 1987.
- [Lorensen and Cline 1987] W. E. Lorensen and H. E. Cline. Marching cubes: a high resolution 3D surface construction algorithm. *Computer Graphics*, **21**:163–170, 1987.
- [Forchhammer 1989] S. Forchhammer. Digital plane and grid point segments. *Computer Vision Graphics Image Processing*, **47**:373–384, 1989.

1990-1999

- [Bruckstein 1991] A. M. Bruckstein. Self-similarity properties of digitized straight lines. *Contemp. Math.*, **119**:1–20, 1991.
- [Kim 1991] C. E. Kim and I. Stojmenović. On the recognition of digital planes in three-dimensional space. *Pattern Recognition Letters*, **12**:665–669, 1991.
- [Reveillès 1991] J.-P. Reveillès. Géométrie discrète, calcul en nombres entiers et algorithmique. Thèse d'état, Univ. Louis Pasteur, Strasbourg, 1991.
- [Stojmenović and Tosić 1991] I. Stojmenović and R. Tosić. Digitization schemes and the recognition of digital straight lines, hyperplanes and flats in arbitrary dimensions. *Vision Geometry, Contemporary Mathematics Series*, **119**:197–212, 1991.
- [Lunnon and Pleasants 1992] W. F. Lunnon and P. A. B. Pleasants. Characterization of two-distance sequences. *J. Australian Mathematical Society, Ser. A*, **53**:198–218, 1992.
- [Lindenbaum and Bruckstein 1993] M. Lindenbaum and A. M. Bruckstein. On recursive, $O(n)$ partitioning of a digitized curve into digital straight segments, *IEEE Trans. Pattern Analysis Machine Intelligence*, **15**:949–953, 1993.
- [Veelaert 1993] P. Veelaert. On the flatness of digital hyperplanes. *J. Math. Imaging and Vision*, **3**:205–221, 1993.
- [Voss 1993] K. Voss. *Discrete Images, Objects, and Functions in \mathbb{Z}^n* . Springer, Berlin, 1993.
- [Debled-Renesson and Reveillès 1994] I. Debled-Renesson and J.-P. Reveillès. A new approach to digital planes. In Proc. *Vision Geometry III*, SPIE 2356, pages 12–21, 1994.
- [Ito and Ohtsuki 1994] S. Ito and M. Ohtsuki. Parallelogram tilings and

- Jacobi-Perron algorithm. *Tokyo J. Math* **17**:33–58, 1994.
- [Veelaert 1994] P. Veelaert. Digital planarity of rectangular surface segments. *IEEE Trans. Pattern Analysis Machine Intelligence*, **16**:647–652, 1994.
- [Debled-Renesson 1995] I. Debled-Renesson. Etude et reconnaissance des droites et plans discrets. *PhD Thesis*, Université Louis Pasteur, Strasbourg, France, 1995.
- [Figueiredo and Reveillès 1995] O. Figueiredo and J.-P. Reveillès. A contribution to 3D digital lines. In Proc. *Discrete Geometry for Computer Imagery*, pages 187–198, 1995.
- [Françon 1995] J. Françon. Arithmetic planes and combinatorial manifolds. In Proc. Int. Workshop *Discrete Geometry for Computer Imagery*, pages 209–217, 1995.
- [Reveillès 1995] J.-P. Reveillès. Combinatorial pieces in digital lines and planes. In Proc. *Vision Geometry IV*, SPIE 2573, pages 23–34, 1995.
- [Fukuda and Prodon 1996] K. Fukuda and A. Prodon. Double description method revisited. In Proc. *Combinatorics and Computer Science*, LNCS 1120, pages 91–111, Springer, Berlin, 1996.
- [Françon et al. 1996] J. Françon, J. M. Schramm, and M. Tajine. Recognizing arithmetic straight lines and planes. In Proc. *Discrete Geometry for Computer Imagery*, LNCS 1176, pages 141–150, Springer, Berlin, 1996.
- [Klette et al. 1996] R. Klette, I. Stojmenović, and J. Žunić. A parametrization of digital planes by least square fits and generalizations. *Graphical Models Image Processing*, **58**:295–300, 1996.
- [Andres et al. 1997] E. Andres, R. Acharya, and C. Sibata. Discrete analytical hyperplanes. *Graphical Models and Image Processing*, **59**:302–309, 1997.
- [Andres et al. 1997a] E. Andres, Ph. Nehlig and J. Françon. Supercover of straight lines, planes and triangles. In Proc. *Discrete Geometry for Computer Imagery*, LNCS 1347, pages 87–98, Springer, Berlin, 1997.
- [Andres et al. 1997b] E. Andres, Ph. Nehlig and J. Françon. Tunnel-free supercover 3D polygons and polyhedra. In Proc. *Eurographics*, pages C3-C13, 1997.
- [Nivat 1997] M. Nivat. Invited talk at ICALP, Bologna 1997.
- [Schramm 1997] J.-M. Schramm. Coplanar tricubes. In Proc. *Discrete Geometry for Computer Imagery*, LNCS 1347, pages 87–98, Springer, Berlin, 1997.
- [Vuillon 1998] L. Vuillon. Combinatoire des motif d’une suite sturmienne bidimensionnelle. *Theoretical Computer Science*, **209**:261–285, 1998.
- [Cassaigne 1999] J. Cassaigne. Two-dimensional sequences of complexity $mn + 1$. *J. Automatic Language Combinatorics*, **4**:153–170, 1999.
- [Françon and Papier 1999] J. Françon and L. Papier. Polyhedrization of the boundary of a voxel object. In Proc. *Discrete Geometry for Computer Imagery*, LNCS 1568, pages 425–434, Springer, Berlin, 1999.
- 2000-...**
- [Berthé and Vuillon 2000a] V. Berthé and L. Vuillon. Tilings and rotations on the torus: a two-dimensional generalization of Sturmian words. *Discrete Mathematics*, **223**:27–53, 2000.

- [Berthé and Vuillon 2000b] V. Berthé and L. Vuillon. Suites doubles de basse complexité. *J. Théor. Nombres Bordeaux*, **12**:179–208, 2000.
- [Barneva et al. 2000] R. P. Barneva, V. E. Brimkov, and Ph. Nehlig. Thin discrete triangular meshes. *Theoretical Computer Science*, **246**:73–105, 2000.
- [Brimkov 2000] V. E. Brimkov. Optimally fast parallel testing 2D-arrays for existence of repetitive patterns. In Proc. *Int. Workshop on Combinatorial Image Analysis*, pages 23–38, 2000.
- [Brimkov et al. 2000a] V. E. Brimkov, E. Andres, and R. P. Barneva. Object discretizations in higher dimensions. In Proc. *Discrete Geometry for Computer Imagery*, LNCS 1953, pages 210–221, Springer, Berlin, 2000.
- [Brimkov et al. 2000b] V. E. Brimkov, R. P. Barneva, and Ph. Nehlig. Minimally thin discrete triangulations. In *Volume Graphics* (A. Kaufman, R. Yagel, and M. Chen, editors), Springer, Chapter 3, pages 51–70, 2000.
- [Lachaud and Montanvert 2000] J.-O. Lachaud and A. Montanvert. Continuous analogs of digital boundaries: A topological approach to iso-surfaces. *Graphical Models and Image Processing*, **62**:129–164, 2000.
- [Vittone and Chassery 2000] J. Vittone and J.-M. Chassery. Recognition of digital naive planes and polyhedrization. In Proc. *Discrete Geometry for Computer Imagery*, LNCS 1953, pages 296–307, Springer, Berlin, 2000.
- [Arnoux et al. 2001] P. Arnoux, V. Berthé, H. Ei, and S. Ito. Tilings, quasicrystals, discrete planes, generalized substitutions, and multidimensional continued fractions. *Discrete Mathematics and Theoretical Computer Science Proc.*, **AA (DM-CCG)**:059–078, 2001.
- [Berthé and Vuillon 2001] V. Berthé and L. Vuillon. Palindromes and two-dimensional Sturmian sequences. *J. Autom. Lang. Comb.*, **6**:121–138, 2001.
- [Klette and Sun 2001] R. Klette and H.-J. Sun. Digital planar segment based polyhedrization for surface area estimation. In Proc. *Visual Form*, pages 356–366. Springer, Berlin, 2001.
- [Rosenfeld and Klette 2001] A. Rosenfeld and R. Klette. Digital straightness. In *Electronic Notes in Theoretical Computer Science* **46**, 2001.
- [Allouche and Shallit] J.-P. Allouche and J. O. Shallit. *Automatic Sequences: Theory and Applications*. Cambridge University Press, 2002.
- [Berthé and Tijdeman 2002] V. Berthé and R. Tijdeman. Balance properties of multi-dimensional words. *Theoretical Computer Science*, **273**:197–224, 2002.
- [Brimkov 2002] V.E. Brimkov. Digital flatness and related combinatorial problems. CITR-TR-120, Computer Science Department, University of Auckland, 2002.
- [Brimkov et al. 2002] V. E. Brimkov, E. Andres, and R. P. Barneva. Object discretizations in higher dimensions. *Pattern Recognition Letters*, **23**:623–636, 2002.
- [Brimkov and Barneva 2002] V. E. Brimkov and R. P. Barneva. Graceful planes and lines. *Theoretical Computer Science*, **283**:151–170, 2002.
- [Buzer 2002] L. Buzer. An incremental linear time algorithm for digital line and plane recognition using a linear incremental feasibility problem. In Proc. *Discrete Geometry for Computer Imagery*, LNCS 2301, pages 372–381,

- Springer, Berlin, 2002.
- [Lothaire 2002] M. Lothaire (ed.). *Algebraic Combinatorics on Words*. Cambridge University Press, Cambridge, 2002.
- [Andres 2003] E. Andres. Discrete linear objects in dimension n : the standard model. *Graphical Models*, **65**:92–111, 2003.
- [Brimkov and Barneva 2003] V. E. Brimkov and R. P. Barneva. Connectivity of discrete planes. CITR-TR-125, Computer Science Department, University of Auckland, 2003.
- [Epifanio et al. 2003] Ch. Epifanio, M. Koskas, and F. Mignosi. On a conjecture on bidimensional words. *Theoretical Computer Science*, **299**:123–150, 2003.
- [Gérard et al. 2003] Y. Gérard, I. Debled-Rennesson, and P. Zimmermann. An elementary digital plane recognition algorithm. In Proc. *Int. Workshop on Combinatorial Image Analysis*, Elsevier ENDM, 2003 (to appear in *Discrete Applied Mathematics*).
- [Brimkov and Barneva 2004] V. E. Brimkov and R. P. Barneva. Connectivity of discrete planes. *Theoretical Computer Science*, **319**:203–227, 2004.
- [Brimkov and Klette 2004] V. E. Brimkov and R. Klette. Curves, hypersurfaces, and good pairs of adjacency relations. In Proc. *Int. Workshop on Combinatorial Image Analysis*, LNCS 3322, pages 425–434, Springer, Berlin, 2004.
- [Coeurjolly et al. 2004] D. Coeurjolly, A. Guillaume, and I. Sivignon. Reversible discrete volume polyhedrization using Marching Cubes simplification. In Proc. *Vision Geometry XII*, SPIE 5300, pages 1-11, 2004.
- [Klette and Rosenfeld 2004] R. Klette and A. Rosenfeld. *Digital Geometry - Geometric Methods for Digital Picture Analysis*. Morgan Kaufmann, San Francisco, 2004.
- [Quas and Zamboni 2004] A. Quas and L.Q. Zamboni. Periodicity and local complexity. *Theoretical Computer Science*, **319**:229–240, 2004.
- [Brimkov and Barneva 2005] V. E. Brimkov and R. P. Barneva. Plane digitization and related combinatorial problems. *Discrete Applied Mathematics* **147**:169–186, 2005.
- [Coeurjolly et al. 2005] D. Coeurjolly, I. Sivignon, F. Dupont, F. Feschet and J.-M. Chassery. On digital plane preimage structure. *Discrete Applied Mathematics*, article in press, 2005.
- [Gérard et al. 2005] Y. Gérard, I. Debled-Rennesson and P. Zimmermann. An elementary digital plane recognition algorithm. *Discrete Applied Mathematics*, article in press, 2005.